Chapter 10

Interactions Between Large and Small Particles

10.1 Multiple Length Scales

The interactions between large and small particles involve multiple length scales. Let a and b denote the size of the large and small particles, respectively, and let h denote a measure of the gap between them. This chapter is concerned with the case where $b \ll h \ll a$ (see Figure 10.1). In essence, whereas the larger particle is in the far field of the smaller one, the smaller particle is in the near field of the larger one, whence a special form of the method of reflections is required. The key idea is that over lengths scales associated with the larger particle, the disturbance fields produced by the smaller one may be approximated by fields produced by equivalent a small number of Stokes singularities. From Chapter 3, we known that the higher order singularities (higher order terms in the multipole expansion) diminish in influence as powers of b/h.

The resistance and mobility functions are obtained by the method of reflections, as in Chapter 8 (see Figure 8.1), but with one crucial difference. For reflections at the larger particle, we retain the entire multipole solution, or

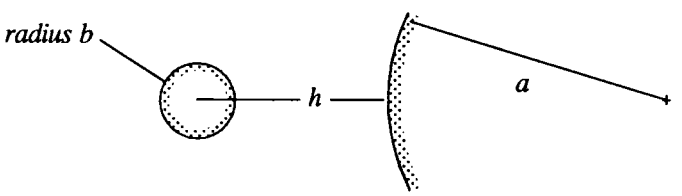

Figure 10.1: The geometry of large-small hydrodynamic interactions.

equivalently, use the exact result for image singularities induced by Stokes singularities near the particle. In practice, such information is available only for simple shapes — such as the sphere, cylinder, and plane wall — so there is a restriction on the shape of the larger particle (or wall-shape). The smaller particle can be of arbitrary shape, since it is represented by a collection of low-order Stokes singularities. We illustrate this point in Section 10.6 and 10.7 by examining the interactions between spheres of radii a and b with $\beta = b/a \ll 1$.

In the next four sections, we derive images for the Stokes singularities near a rigid sphere and spherical drop. In the next section, we consider the image system for a Stokeslet. The analysis differs for the axisymmetric case (Stokeslet directed along the line of centers) and the transverse case. In Section 10.3, these ideas are extended to spherical drops. The images for the higher order singularities (Stokes dipoles) are derived in Section 10.4 by superposition of images of two Stokeslets. The images for the stresslet derived therein are of particular importance in the calculation of resistance and mobility functions. In Section 10.5, we derive the image for the degenerate quadrupole, since it is an important entity in the singularity representation for spheres.

10.2 Image System for the Stokeslet Near a Rigid Sphere

Consider a Stokeslet at $\boldsymbol{x}_2$ and a sphere of radius a centered at $\boldsymbol{x}_1$, as shown in Figure 10.2. We simplify the notation by scaling lengths with the sphere radius a. Our task is to find the solution to the following problem:

$$-\nabla p + \mu\nabla^2 \boldsymbol{v} = -\boldsymbol{F}\delta(\boldsymbol{x} - \boldsymbol{x}_2), \qquad \nabla \cdot \boldsymbol{v} = 0, \tag{10.1}$$

with $|\boldsymbol{x}_2 - \boldsymbol{x}_1| > 1$ and the boundary conditions,

$$\boldsymbol{v} = 0 \qquad \text{for } r = a\,, \qquad\qquad \boldsymbol{v} \to 0 \qquad \text{as } r \to \infty,$$

with $r = |\boldsymbol{x} - \boldsymbol{x}_1|$.

We first write the solution as

$$\boldsymbol{v} = \boldsymbol{F} \cdot \mathcal{G}(\boldsymbol{x} - \boldsymbol{x}_2)/(8\pi\mu) + \boldsymbol{v}^*\,, \tag{10.2}$$

i.e., $\boldsymbol{v}^*$ is the image field. The essential steps in the solution procedure are as follows:

1. The Stokeslet at $\boldsymbol{x}_2$ is first written in terms of spherical harmonics, which are then transformed into harmonics based at $\boldsymbol{x}_1$ by an application of the addition theorem [30].

2. The image system is expanded as a multipole series about $\boldsymbol{x}_1$, and it too is rewritten in terms of the spherical harmonics at $\boldsymbol{x}_1$.

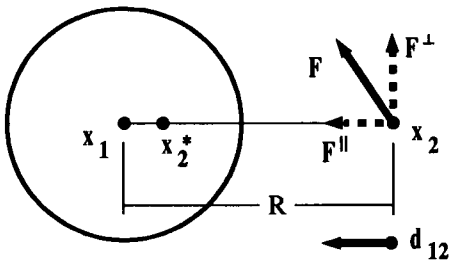

Figure 10.2: The Stokeslet-sphere geometry.

3. The coefficients in the image system may be determined by matching the boundary conditions at the sphere surface (term by term). In this case, we have the no-slip condition, while for viscous drops we use the more general boundary conditions described in Chapter 4.

If desired, the multipole expansion can be converted (by solving the appropriate set of moment equations) into a singularity solution. It turns out that the image system is the line between $\boldsymbol{x}_1$ and $\boldsymbol{x}_2^*$.

We start with the representation for the Stokeslet:

$$F_j \mathcal{G}_{ij} = F_i \frac{1}{r_2} + F_j (x - x_2)_i \frac{\partial}{\partial x_{2j}} \frac{1}{r_2} , \tag{10.3}$$

where we define $r_\alpha = |\boldsymbol{x} - \boldsymbol{x}_\alpha|$. Now harmonics about $\boldsymbol{x}_2$ may be recast in terms of those at $\boldsymbol{x}_1$ by the Legendre expansion,

$$\frac{1}{r_2} = \sum_{n=0}^{\infty} \frac{r_1^{2n+1}}{R^{n+1}} \frac{(\boldsymbol{d}_{12} \cdot \nabla)^n}{n!} \frac{1}{r_1} , \tag{10.4}$$

with the vector $\boldsymbol{d}_{12}$ defined by[1] $\boldsymbol{d}_{12} = (\boldsymbol{x}_1 - \boldsymbol{x}_2)/R$, $R = |\boldsymbol{x}_2 - \boldsymbol{x}_1| > 1$. Thus the Stokeslet at $\boldsymbol{x}_2$ may be written in terms of harmonics centered at $\boldsymbol{x}_1$,

$$\begin{aligned} F_j \mathcal{G}_{ij} &= F_i \sum_{n=0}^{\infty} \frac{r_1^{2n+1}}{R^{n+1}} \frac{(\boldsymbol{d}_{12} \cdot \nabla)^n}{n!} \frac{1}{r_1} \\ &+ (\boldsymbol{x} - \boldsymbol{x}_1)_i \, F_j \frac{\partial}{\partial x_{2j}} \sum_{n=0}^{\infty} \frac{r_1^{2n+1}}{R^{n+1}} \frac{(\boldsymbol{d}_{12} \cdot \nabla)^n}{n!} \frac{1}{r_1} \\ &- (\boldsymbol{x}_2 - \boldsymbol{x}_1)_i \, F_j \frac{\partial}{\partial x_{2j}} \sum_{n=0}^{\infty} \frac{r_1^{2n+1}}{R^{n+1}} \frac{(\boldsymbol{d}_{12} \cdot \nabla)^n}{n!} \frac{1}{r_1} , \end{aligned} \tag{10.5}$$

where $\partial/\partial x_{2j}$ denotes the nabla operator with respect to $\boldsymbol{x}_2$. The nabla operation with respect to $\boldsymbol{x}_2$ may be performed by noting that

$$\nabla_2 R^{-(n+1)} = -(n+1) R^{-(n+2)} (\boldsymbol{x}_2 - \boldsymbol{x}_1)/R = (n+1) R^{-(n+2)} \boldsymbol{d}_{12} \tag{10.6}$$

[1]When written in index notation, the subscripts (12) in $\boldsymbol{d}_{12}$ will be omitted.

and that $(\boldsymbol{d}_{12} \cdot \nabla_2)\boldsymbol{d}_{12} = \mathbf{0}$.

At this point, it is convenient to consider separately the two cases: $\boldsymbol{F}$ parallel to $\boldsymbol{d}_{12}$ (which is an axisymmetric problem) and $\boldsymbol{F}$ perpendicular to $\boldsymbol{d}_{12}$.

10.2.1 The Axisymmetric Stokeslet

For this case, we write $\boldsymbol{F} = F\boldsymbol{d}_{12}$ and Equation 10.6 becomes

$$\begin{aligned} Fd_j\mathcal{G}_{ij} &= Fd_i \sum_{n=0}^{\infty} (n+2)\frac{r_1^{2n+1}}{R^{n+1}} \frac{(\boldsymbol{d}_{12}\cdot\nabla)^n}{n!}\frac{1}{r_1} \\ &+ F(\boldsymbol{x}-\boldsymbol{x}_1)_i \sum_{n=0}^{\infty} (n+1)\frac{r_1^{2n+1}}{R^{n+2}} \frac{(\boldsymbol{d}_{12}\cdot\nabla)^n}{n!}\frac{1}{r_1}\,. \end{aligned} \tag{10.7}$$

Thus the Stokeslet at $\boldsymbol{x}_2$ has been expressed in terms of harmonics centered at $\boldsymbol{x}_1$.

We write the image system, $\boldsymbol{v}^*$, as a multipole expansion:

$$\boldsymbol{v}^* = \frac{F\boldsymbol{d}_{12}}{8\pi\mu} \sum_{n=0}^{\infty} \left\{ A_n^{\parallel} \frac{(\boldsymbol{d}_{12}\cdot\nabla)^n}{n!}\mathcal{G}_{ij}(\boldsymbol{x}-\boldsymbol{x}_1) + B_n^{\parallel}\frac{(\boldsymbol{d}_{12}\cdot\nabla)^n}{n!}\nabla^2\mathcal{G}_{ij}(\boldsymbol{x}-\boldsymbol{x}_1) \right\}.$$

The assumed form follows as a consequence of axisymmetry in the flow field (see Exercise 4.2).

These Stokes multipoles may be written as

$$\frac{(\boldsymbol{d}_{12}\cdot\nabla)^n}{n!}\mathcal{G}_{ij}(\boldsymbol{x}-\boldsymbol{x}_1) = \frac{(\boldsymbol{d}_{12}\cdot\nabla)^n}{n!}\left\{\delta_{ij}\frac{1}{r_1} - (\boldsymbol{x}-\boldsymbol{x}_1)_i\frac{\partial}{\partial x_j}\frac{1}{r_1}\right\},$$

which, since only two terms are nonzero when the Leibniz product rule is applied, simplifies to

$$\begin{aligned} \frac{(\boldsymbol{d}_{12}\cdot\nabla)^n}{n!}\mathcal{G}_{ij}(\boldsymbol{x}-\boldsymbol{x}_1) &= \delta_{ij}\frac{(\boldsymbol{d}_{12}\cdot\nabla)^n}{n!}\frac{1}{r_1} \\ &- (\boldsymbol{x}-\boldsymbol{x}_1)_i\frac{\partial}{\partial x_j}\frac{(\boldsymbol{d}_{12}\cdot\nabla)^n}{n!}\frac{1}{r_1} \\ &- d_i\frac{\partial}{\partial x_j}\frac{(\boldsymbol{d}_{12}\cdot\nabla)^{n-1}}{(n-1)!}\frac{1}{r_1}\,. \end{aligned} \tag{10.8}$$

The $B_n^{\parallel}$ terms may be rewritten in terms of vector harmonics by recalling that $\nabla^2\mathcal{G}(\boldsymbol{x}) = -2\nabla\nabla r^{-1}$. Thus the image system may be written as

$$\begin{aligned} v_i^* &= \frac{F}{8\pi\mu}\sum_{n=0}^{\infty}\left\{ A_n^{\parallel}\left[(1-n)d_i\frac{(\boldsymbol{d}_{12}\cdot\nabla)^n}{n!}\frac{1}{r_1} - (\boldsymbol{x}-\boldsymbol{x}_1)_i\frac{(\boldsymbol{d}_{12}\cdot\nabla)^{n+1}}{8\pi\mu n!}\frac{1}{r_1}\right]\right. \\ &\left. - 2B_n^{\parallel}\frac{(\boldsymbol{d}_{12}\cdot\nabla)^{n+1}}{n!}\frac{\partial}{\partial x_i}\frac{1}{r_1}\right\}. \end{aligned} \tag{10.9}$$

We can determine the coefficients $A_n^{\parallel}$ and $B_n^{\parallel}$ from the boundary conditions by collecting terms in harmonics of each order in Equations 10.8 and 10.9.

However, these harmonics are not independent; for example, we may eliminate terms involving $\boldsymbol{d}_{12}(\boldsymbol{d}_{12}\cdot\nabla)^n(1/r_1)$ by using the identity

$$\begin{aligned}\boldsymbol{d}_{12}(\boldsymbol{d}_{12}\cdot\nabla)^n\frac{1}{r_1} &= \frac{-r_1^2}{(2n+1)(n+1)}\nabla(\boldsymbol{d}_{12}\cdot\nabla)^{n+1}\frac{1}{r_1}\\ &+ \frac{n}{2n+1}\nabla(\boldsymbol{d}_{12}\cdot\nabla)^{n-1}\frac{1}{r_1}\\ &- \frac{(2n+3)}{(2n+1)(n+1)}(\boldsymbol{x}-\boldsymbol{x}_1)(\boldsymbol{d}_{12}\cdot\nabla)^{n+1}\frac{1}{r_1}\,.\end{aligned}$$

Thus at $r_1 = 1$, the expansion for the Stokeslet becomes

$$\begin{aligned}Fd_j\mathcal{G}_{ij} &= F\sum_{n=0}^{\infty}\frac{(n+3)}{(2n+3)R^{n+2}}\frac{\partial}{\partial x_i}\frac{(\boldsymbol{d}_{12}\cdot\nabla)^n}{n!}\frac{1}{r_1}\\ &- F\sum_{n=1}^{\infty}\frac{(n+1)}{(2n-1)R^n}\frac{\partial}{\partial x_i}\frac{(\boldsymbol{d}_{12}\cdot\nabla)^n}{n!}\frac{1}{r_1}\\ &+ F(\boldsymbol{x}-\boldsymbol{x}_1)_i\sum_{n=0}^{\infty}\frac{(n+1)}{R^{n+2}}\frac{(\boldsymbol{d}_{12}\cdot\nabla)^n}{n!}\frac{1}{r_1}\\ &- F(\boldsymbol{x}-\boldsymbol{x}_1)_i\sum_{n=1}^{\infty}\frac{(n+1)(2n+1)}{(2n-1)R^n}\frac{(\boldsymbol{d}_{12}\cdot\nabla)^n}{n!}\frac{1}{r_1}\,.\end{aligned}$$

Note that the two terms with $n = 0$ cancel, so we may start all four summations from $n = 1$. Similarly, the expansion for the image system becomes

$$\begin{aligned}v_i^* &= -\frac{F}{8\pi\mu}\sum_{n=1}^{\infty}\frac{2(n+1)}{(2n-1)}A_{n-1}^{\parallel}(\boldsymbol{x}-\boldsymbol{x}_1)_i\frac{(\boldsymbol{d}_{12}\cdot\nabla)^n}{n!}\frac{1}{r_1}\\ &+ \frac{F}{8\pi\mu}\sum_{n=1}^{\infty}\Big[\frac{(n-2)}{(2n-1)}A_{n-1}^{\parallel} - \frac{n}{(2n+3)}A_{n+1}^{\parallel}\\ &\qquad - 2nB_{n-1}^{\parallel}\Big]\frac{\partial}{\partial x_i}\frac{(\boldsymbol{d}_{12}\cdot\nabla)^n}{n!}\frac{1}{r_1}\,.\end{aligned}$$

We collect terms in $(\boldsymbol{x}-\boldsymbol{x}_1)(\boldsymbol{d}_{12}\cdot\nabla)^n(1/r_1)$ and $\nabla(\boldsymbol{d}_{12}\cdot\nabla)^n(1/r_1)$ and set each equal to zero. Thus for $n \geq 1$, we have

$$\begin{aligned}\frac{2(n+1)}{2n-1}A_{n-1}^{\parallel} &= (n+1)R^{-(n+2)} - \frac{(n+1)(2n+1)}{2n-1}R^{-n}\\ \frac{nA_{n+1}^{\parallel}}{2n+3} - \frac{(n-2)}{(2n-1)}A_{n-1}^{\parallel} - 2nB_{n-1}^{\parallel} &= \frac{n+3}{2n+3}R^{-(n+2)} - \frac{n+1}{2n-1}R^{-n}\,,\end{aligned}$$

which lead to

$$A_n^{\parallel} = -(n+\frac{3}{2})R^{-(n+1)} + (n+\frac{1}{2})R^{-(n+3)} \tag{10.10}$$

$$B_n^{\parallel} = -\frac{1}{4}(1-R^2)^2R^{-(n+5)}\,. \tag{10.11}$$

In the multipole expansion, the coefficient of the monopole field is the hydrodynamic force exerted on the sphere, *i.e.*,

$$\boldsymbol{F}^{\mathrm{Hyd}} = -A_0^{\parallel} F \boldsymbol{d}_{12} = \left(\frac{3}{2}R^{-1} - \frac{1}{2}R^{-3}\right) F \boldsymbol{d}_{12} \,, \tag{10.12}$$

while the coefficient of the Stokes dipole, which in this case is symmetric, must be the stresslet, so that

$$\boldsymbol{S} = A_1^{\parallel} F \boldsymbol{d}_{12} = \left(-\frac{5}{2}R^{-2} + \frac{3}{2}R^{-4}\right) F \boldsymbol{d}_{12}\boldsymbol{d}_{12} \,. \tag{10.13}$$

These results are consistent with that obtained by applying the Faxén laws for the force and stresslet to the ambient field, $\boldsymbol{F} \cdot \mathcal{G}(\boldsymbol{x} - \boldsymbol{x}_2)/(8\pi\mu)$.

10.2.2 The Transverse Stokeslet

We now consider the transverse case with $\boldsymbol{F} \cdot \boldsymbol{d}_{12} = 0$. Equation 10.6 becomes

$$\begin{aligned} F_j \mathcal{G}_{ij} &= F_i \sum_{n=0}^{\infty} \frac{r_1^{2n+1}}{R^{n+1}} \frac{(\boldsymbol{d}_{12} \cdot \nabla)^n}{n!} \frac{1}{r_1} \\ &- (\boldsymbol{x} - \boldsymbol{x}_1)_i \sum_{n=1}^{\infty} \frac{r_1^{2n+1}}{R^{n+2}} (\boldsymbol{F} \cdot \nabla) \frac{(\boldsymbol{d}_{12} \cdot \nabla)^{n-1}}{(n-1)!} \frac{1}{r_1} \\ &- d_i \sum_{n=1}^{\infty} \frac{r_1^{2n+1}}{R^{n+1}} (\boldsymbol{F} \cdot \nabla) \frac{(\boldsymbol{d}_{12} \cdot \nabla)^{n-1}}{(n-1)!} \frac{1}{r_1} \,. \end{aligned} \tag{10.14}$$

The Stokeslet at $\boldsymbol{x}_2$ has been expressed in terms of harmonics centered at $\boldsymbol{x}_1$.

We write the image system for the transverse case as follows:

$$\begin{aligned} v_i^* &= \frac{F_j}{8\pi\mu} \sum_{n=0}^{\infty} \left\{ A_n^{\perp} \frac{(\boldsymbol{d}_{12} \cdot \nabla)^n}{n!} \mathcal{G}_{ij}(\boldsymbol{x} - \boldsymbol{x}_1) + B_n^{\perp} \frac{(\boldsymbol{d}_{12} \cdot \nabla)^n}{n!} \nabla^2 \mathcal{G}_{ij}(\boldsymbol{x} - \boldsymbol{x}_1) \right\} \\ &+ \frac{\epsilon_{ijk} t_j}{8\pi\mu} \sum_{n=0}^{\infty} C_n^{\perp} \frac{(\boldsymbol{d}_{12} \cdot \nabla)^n}{n!} \frac{\partial}{\partial x_k} \frac{1}{r_1} \,. \end{aligned} \tag{10.15}$$

Here, $\boldsymbol{t} = \boldsymbol{F} \times \boldsymbol{d}_{12}$ and the $C_n^{\perp}$ terms originate because the Stokeslet at $\boldsymbol{x}_2$ is not pointed along the axis of symmetry. These terms may also be expressed as derivatives of the rotlet using the identity

$$\begin{aligned} \epsilon_{ijk} t_j \frac{\partial}{\partial x_k} \frac{1}{r_1} &= \frac{1}{2} \epsilon_{jkl} t_j \mathcal{G}_{il,k}(\boldsymbol{x} - \boldsymbol{x}_1) \\ &= \frac{1}{2}(F_k d_j - F_j d_k) \mathcal{G}_{ij,k}(\boldsymbol{x} - \boldsymbol{x}_1) \\ &= (F_k d_i - F_i d_k) \frac{\partial}{\partial x_k} \frac{1}{r_1} \,. \end{aligned} \tag{10.16}$$

Equation 10.16 may be used to convert harmonics in Equation 10.14 of the form $\boldsymbol{d}_{12}(\boldsymbol{F} \cdot \nabla)(\boldsymbol{d}_{12} \cdot \nabla)^{n-1}(1/r_1)$ to terms of the form $\boldsymbol{F}(\boldsymbol{d}_{12} \cdot \nabla)^n(1/r_1)$ plus

derivatives of the rotlet. The image system may then be written as

$$\begin{aligned} v_i^* &= \sum_{n=0}^{\infty} A_n^{\perp} \Big[F_i(1-n)\frac{(\boldsymbol{d}_{12}\cdot\nabla)^n}{8\pi\mu\, n!}\frac{1}{r_1} - (\boldsymbol{x}-\boldsymbol{x}_1)_i(\boldsymbol{F}\cdot\nabla)\frac{(\boldsymbol{d}_{12}\cdot\nabla)^n}{8\pi\mu\, n!}\frac{1}{r_1} \\ &\qquad - n(\boldsymbol{t}\times\nabla)_i\frac{(\boldsymbol{d}_{12}\cdot\nabla)^{n-1}}{8\pi\mu\, n!}\frac{1}{r_1}\Big] \\ &\quad - \sum_{n=0}^{\infty} 2B_n^{\perp}\frac{\partial}{\partial x_i}(\boldsymbol{F}\cdot\nabla)\frac{(\boldsymbol{d}_{12}\cdot\nabla)^n}{8\pi\mu\, n!}\frac{\partial}{\partial x_i}\frac{1}{r_1} \\ &\quad + \sum_{n=0}^{\infty} C_n^{\perp}(\boldsymbol{t}\times\nabla)_i\frac{(\boldsymbol{d}_{12}\cdot\nabla)^n}{8\pi\mu\, n!}\frac{1}{r_1}\,. \end{aligned} \tag{10.17}$$

Since we have "three" coefficients — $A_n^{\perp}$, $B_n^{\perp}$, and $C_n^{\perp}$ — we should collect terms in three linearly independent vector functions. We have already mentioned how (using Equation 10.16) one of the vector functions may be eliminated. An examination of Equations 10.14 and 10.17 reveals that this still leaves four types. However, for $\boldsymbol{F}\cdot\boldsymbol{d}_{12}=0$ we have on the surface $r_1=1$ the identity,

$$\begin{aligned} &(\boldsymbol{x}-\boldsymbol{x}_1)(\boldsymbol{F}\cdot\nabla)(\boldsymbol{d}_{12}\cdot\nabla)^n\frac{1}{r_1} \\ &= \frac{-1}{(2n+3)}\nabla(\boldsymbol{F}\cdot\nabla)(\boldsymbol{d}_{12}\cdot\nabla)^n\frac{1}{r_1} + \frac{n(n-1)}{(2n+3)}\nabla(\boldsymbol{F}\cdot\nabla)(\boldsymbol{d}_{12}\cdot\nabla)^{n-2}\frac{1}{r_1} \\ &- \frac{(2n+1)(n+1)}{(2n+3)}\boldsymbol{F}(\boldsymbol{d}_{12}\cdot\nabla)^n\frac{1}{r_1} \\ &- \frac{n(2n+1)}{(2n+3)}(\boldsymbol{t}\times\nabla)(\boldsymbol{d}_{12}\cdot\nabla)^{n-1}\frac{1}{r_1}\,. \end{aligned}$$

Therefore, the final expressions for the Stokeslet and the image system involve three basis functions. For example, the Stokeslet may be written as

$$\begin{aligned} F_j\mathcal{G}_{ij} &= F_i\sum_{n=0}^{\infty}\Big[(1-n)R^{-(n+1)} + \frac{(2n+1)(n+1)}{(2n+3)R^{n+3}}\Big]\frac{(\boldsymbol{d}_{12}\cdot\nabla)^n}{n!}\frac{1}{r_1} \\ &\quad + \sum_{n=0}^{\infty}\Big[\frac{R^{-(n+3)}}{(2n+3)} - \frac{R^{-(n+5)}}{(2n+7)}\Big]\frac{\partial}{\partial x_i}(\boldsymbol{F}\cdot\nabla)\frac{(\boldsymbol{d}_{12}\cdot\nabla)^n}{n!}\frac{1}{r_1} \\ &\quad - \sum_{n=0}^{\infty}\Big[R^{-(n+2)} - \frac{(2n+3)}{(2n+5)}R^{-(n+4)}\Big](\boldsymbol{t}\times\nabla)_i\frac{(\boldsymbol{d}_{12}\cdot\nabla)^n}{n!}\frac{1}{r_1}\,. \end{aligned}$$

As before, we determine the coefficients $A_n^{\perp}$, $B_n^{\perp}$, and $C_n^{\perp}$ from the boundary conditions by collecting terms in like harmonics. The terms in $\boldsymbol{F}(\boldsymbol{d}_{12}\cdot\nabla)^n(1/r_1)$, $\nabla(\boldsymbol{F}\cdot\nabla)(\boldsymbol{d}_{12}\cdot\nabla)^n(1/r_1)$, and $(\boldsymbol{t}\times\nabla)(\boldsymbol{d}_{12}\cdot\nabla)^n(1/r_1)$ yield the following set of equations:

$$\begin{aligned} \Big[1-n+\frac{(2n+1)(n+1)}{(2n+3)}\Big]A_n^{\perp} &= \frac{(n-1)}{R^{n+1}} + \frac{(2n+1)(n+1)}{(2n+3)R^{n+3}} \\ \frac{A_n^{\perp}}{(2n+3)} - \frac{A_{n+2}^{\perp}}{(2n+7)} - 2B_n^{\perp} &= -\frac{R^{-(n+3)}}{(2n+3)} + \frac{R^{-(n+5)}}{(2n+7)} \end{aligned}$$

$$\left[-1+\frac{(2n+3)}{(2n+5)}\right]A_{n+1}^{\perp}+C_n^{\perp} \;=\; R^{-(n+2)}-\frac{(2n+3)}{(2n+5)}R^{-(n+4)}\;,$$

which lead to

$$A_n^{\perp} \;=\; \frac{(n-1)(2n+3)}{2(n+2)}R^{-(n+1)}-\frac{(n+1)(2n+1)}{2(n+2)}R^{-(n+3)} \tag{10.18}$$

$$\begin{aligned} B_n^{\perp} \;&=\; \frac{n-1}{4(n+2)}R^{-(n+1)}-\frac{n^2+3n-1}{2(n+2)(n+4)}R^{-(n+3)} \\ &+\; \frac{n+1}{4(n+4)}R^{-(n+5)} \end{aligned} \tag{10.19}$$

$$C_n^{\perp} \;=\; \frac{2n+3}{n+3}R^{-(n+2)}-\frac{2n+3}{n+3}R^{-(n+4)}\;. \tag{10.20}$$

The force, torque, and stresslet exerted by the fluid on the sphere are

$$\boldsymbol{F}^{\mathrm{Hyd}} \;=\; -A_0^{\perp}\boldsymbol{F}=\left(\frac{3}{4}R^{-1}+\frac{1}{4}R^{-3}\right)\boldsymbol{F} \tag{10.21}$$

$$\boldsymbol{T}^{\mathrm{Hyd}} \;=\; (C_0^{\perp}-A_1^{\perp})\boldsymbol{t}=R^{-2}\boldsymbol{F}\times\boldsymbol{d}_{12} \tag{10.22}$$

$$\boldsymbol{S} \;=\; A_1^{\perp}\frac{1}{2}(\boldsymbol{F}\boldsymbol{d}_{12}+\boldsymbol{d}_{12}\boldsymbol{F})=-\frac{1}{2}R^{-4}(\boldsymbol{F}\boldsymbol{d}_{12}+\boldsymbol{d}_{12}\boldsymbol{F})\;. \tag{10.23}$$

Again, these results are consistent with the Faxén laws (see Exercise 10.1).

10.2.3 Singularity Solutions for the Image of a Stokeslet

We have obtained analytic expressions for the image of a Stokeslet near a sphere. As the Stokeslet is placed nearer to the sphere, the contribution from the higher order singularities becomes important. On the other hand, it would be nice to have the option of not dealing with the higher order Stokes singularities; these are awkward to implement in numerical schemes and are not as readily identified with physical quantities. Indeed, a Stokeslet placed very close to the sphere surface corresponds to, in the limit of vanishingly small separations, a Stokeslet near a plane wall. This limiting behavior is difficult to attain as long as the sphere center remains as a parameter in the problem. We would be trying to perform a multipole expansion about a point at infinity!

Here, we show that the image is indeed just a line distribution of a small collection of the lower order Stokes singularities. The line segment runs along the sphere-Stokeslet axis from the sphere center to the inverse point, $\boldsymbol{x}_2^*$, defined by $|\boldsymbol{x}_2^*-\boldsymbol{x}_1|=|\boldsymbol{x}_2-\boldsymbol{x}_1|^{-1}$. In Chapter 12, we will show that in the limit of vanishingly small separations, the contribution from the inverse point dominates and the image for the sphere reduces to the Lorentz image for the plane wall.

The Axisymmetric Problem

Consider a representation of the image system of the form

$$\boldsymbol{v}^* = -\boldsymbol{d}_{12}\cdot\int_0^{1/R} f(\xi)\frac{\mathcal{G}(\boldsymbol{x}-\boldsymbol{\xi})}{8\pi\mu}\,d\xi \;-\; \boldsymbol{d}_{12}\cdot\int_0^{1/R} g(\xi)\nabla^2\frac{\mathcal{G}(\boldsymbol{x}-\boldsymbol{\xi})}{8\pi\mu}\,d\xi\;,$$

where ξ lies on the line between $\boldsymbol{x}_1$ and $\boldsymbol{x}_2$. Now for any ξ in this interval, we have the Taylor expansion about $\boldsymbol{\xi} = \boldsymbol{x}_1$,

$$\mathcal{G}(\boldsymbol{x} - \boldsymbol{\xi}) = \sum_{n=0}^{\infty} \xi^n \frac{(\boldsymbol{d}_{12} \cdot \nabla)^n}{n!} \mathcal{G}(\boldsymbol{x} - \boldsymbol{x}_1) \ .$$

Therefore, the line distribution can also be written as a multipole expansion,

$$\begin{aligned} \boldsymbol{v}^* &= -\boldsymbol{d}_{12} \cdot \sum_{n=0}^{\infty} \left[\int_0^{1/R} f(\xi) \xi^n d\xi \right] \frac{(\boldsymbol{d}_{12} \cdot \nabla)^n}{n!} \frac{\mathcal{G}(\boldsymbol{x} - \boldsymbol{\xi})}{8\pi\mu} \, d\xi \\ &- \boldsymbol{d}_{12} \cdot \sum_{n=0}^{\infty} \left[\int_0^{1/R} g(\xi) \xi^n d\xi \right] \frac{(\boldsymbol{d}_{12} \cdot \nabla)^n}{n!} \nabla^2 \frac{\mathcal{G}(\boldsymbol{x} - \boldsymbol{\xi})}{8\pi\mu} \, d\xi \ . \end{aligned}$$

The line representation and the multipole expansion form derived earlier are equivalent if and only if

$$-A_n^{\parallel} = (n + \frac{3}{2}) R^{-(n+1)} - (n + \frac{1}{2}) R^{-(n+3)} = \int_0^{1/R} f(\xi) \xi^n \, d\xi$$

and

$$-B_n^{\parallel} = \frac{1}{4}(1 - R^2)^2 R^{-(n+5)} = \int_0^{1/R} g(\xi) \xi^n \, d\xi \ ,$$

for all $n \geq 0$.

These equations yield the following solution for $f(\xi)$ and $g(\xi)$:

$$\begin{aligned} f(\xi) &= (\frac{3}{2} R^{-1} - \frac{1}{2} R^{-3}) \delta(\xi - R^{-1}) - (R^{-2} - R^{-4}) \frac{\partial}{\partial \xi} \delta(\xi - R^{-1}) \\ g(\xi) &= \frac{1}{4} R^{-5} (1 - R^2)^2 \delta(\xi - R^{-1}) \ , \end{aligned}$$

when we exploit the following identities for generalized functions:

$$\begin{aligned} \int_0^{1/R} \delta(\xi - R^{-1}) \xi^n \, d\xi &= R^{-n} \\ \int_0^{1/R} \frac{\partial}{\partial \xi} \delta(\xi - R^{-1}) \xi^n \, d\xi &= -n R^{-(n-1)} \ . \end{aligned}$$

We insert the result for $f(\xi)$ and $g(\xi)$ to obtain the following image for a Stokeslet oriented along the axis:

$$\begin{aligned} \boldsymbol{v}^* &= -(\frac{3}{2} R^{-1} - \frac{1}{2} R^{-3}) F \boldsymbol{d}_{12} \cdot \frac{\mathcal{G}(\boldsymbol{x} - \boldsymbol{x}_2^*)}{8\pi\mu} \\ &- [(R^{-2} - R^{-4}) F (\boldsymbol{d}_{12} \boldsymbol{d}_{12} - \frac{1}{3} \boldsymbol{\delta}) \cdot \nabla] \cdot \frac{\mathcal{G}(\boldsymbol{x} - \boldsymbol{x}_2^*)}{8\pi\mu} \\ &- \frac{1}{4} R^{-1} (1 - R^{-2})^2 F \boldsymbol{d}_{12} \cdot \nabla^2 \frac{\mathcal{G}(\boldsymbol{x} - \boldsymbol{x}_2^*)}{8\pi\mu} \ . \end{aligned} \tag{10.24}$$

So for the axisymmetric problem the "line distribution" is actually confined to the inverse point, and the collection of singularities consists of a Stokeslet of strength $(\frac{3}{2} R^{-1} - \frac{1}{2} R^{-3})$, a stresslet of strength $(R^{-2} - R^{-4})$, and a degenerate quadrupole of strength $\frac{1}{4} R^{-1} (1 - R^{-2})^2$.

The Transverse Problem

Consider a representation of the image system of the form

$$\begin{aligned} \boldsymbol{v}^* &= -\boldsymbol{F}\cdot\int_0^{1/R} f(\xi)\frac{\mathcal{G}(\boldsymbol{x}-\boldsymbol{\xi})}{8\pi\mu}\,d\xi - \boldsymbol{F}\cdot\int_0^{1/R} g(\xi)\nabla^2\frac{\mathcal{G}(\boldsymbol{x}-\boldsymbol{\xi})}{8\pi\mu}\,d\xi \\ &+ \frac{\boldsymbol{F}\times\boldsymbol{d}_{12}}{8\pi\mu}\times\nabla\int_0^{1/R}\frac{h(\xi)\,d\xi}{|\boldsymbol{x}-\boldsymbol{\xi}|}\,, \end{aligned}$$

where $\boldsymbol{\xi}$ lies on the $\boldsymbol{d}_{12}$ axis as before.

We rewrite the solution for $A_n^\perp$, $B_n^\perp$, and $C_n^\perp$, which was derived earlier as

$$\begin{aligned} A_n^\perp &= (R^{-2}-R^{-4})nR^{-(n-1)} - (\frac{3}{2}R^{-1}-\frac{1}{2}R^{-3})R^{-n} + \frac{3}{2}(R-R^{-1})\frac{R^{-(n+2)}}{(n+2)} \\ B_n^\perp &= \frac{1}{4}(R^{-1}-2R^{-3}+R^{-5})R^{-n} - \frac{3}{4}(R-R^{-1})\frac{R^{-(n+2)}}{(n+2)} \\ &\quad + \frac{3}{4}(R-R^{-1})\frac{R^{-(n+4)}}{(n+4)} \\ C_n^\perp &= 2(R^{-2}-R^{-4})R^{-n} - 3(R-R^{-1})\frac{R^{-(n+3)}}{(n+3)}\,, \end{aligned}$$

to facilitate the identification of the density functions. Terms of the form $R^{-(n+k)}/(n+k)$ appearing above correspond to a true line distribution along $0 \le \xi \le R^{-1}$ with density ξ^{k-1}.

Following the experience from the axisymmetric problem, we make assignments of the form

$$\begin{aligned} -A_n^\perp &= \int_0^{1/R} f(\xi)\xi^n\,d\xi \\ -B_n^\perp &= \int_0^{1/R} g(\xi)\xi^n\,d\xi \\ C_n^\perp &= \int_0^{1/R} h(\xi)\xi^n\,d\xi\,, \end{aligned}$$

for all $n \ge 0$. The solutions for $f(\xi)$, $g(\xi)$, and $h(\xi)$ are

$$\begin{aligned} f(\xi) &= (R^{-2}-R^{-4})\frac{\partial}{\partial\xi}\delta(\xi-R^{-1}) + (\frac{3}{2}R^{-1}-\frac{1}{2}R^{-3})\delta(\xi-R^{-1}) \\ &\quad - \frac{3}{2}(R-R^{-1})\xi \\ g(\xi) &= -\frac{1}{4}(R^{-1}-2R^{-3}+R^{-5})\delta(\xi-R^{-1}) + \frac{3}{4}(R-R^{-1})(\xi-\xi^3) \\ h(\xi) &= 2(R^{-2}-R^{-4})\delta(\xi-R^{-1}) - 3(R-R^{-1})\xi^2\,, \end{aligned}$$

and the image may be written as

$$\boldsymbol{v}^* = -(\frac{3}{2}R^{-1}-\frac{1}{2}R^{-3})\boldsymbol{F}\cdot\frac{\mathcal{G}(\boldsymbol{x}-\boldsymbol{x}_2^*)}{8\pi\mu} + [(R^{-2}-R^{-4})\boldsymbol{F}(\boldsymbol{d}_{12}\cdot\nabla)]\cdot\frac{\mathcal{G}(\boldsymbol{x}-\boldsymbol{x}_2^*)}{8\pi\mu}$$

$$
\begin{aligned}
&+ \frac{1}{4}R^{-1}(1-R^{-2})^2\boldsymbol{F}\cdot\frac{\nabla^2\mathcal{G}(\boldsymbol{x}-\boldsymbol{x}_2^*)}{8\pi\mu} + 2R^{-2}(1-R^{-2})\frac{\boldsymbol{F}\times\boldsymbol{d}_{12}}{8\pi\mu}\times\nabla\frac{1}{|\boldsymbol{x}-\boldsymbol{x}_2^*|} \\
&- \frac{3}{4}(R-R^{-1})\int_0^{1/R}(\xi-\xi^3)\boldsymbol{F}\cdot\nabla^2\frac{\mathcal{G}(\boldsymbol{x}-\boldsymbol{\xi})}{8\pi\mu}\,d\xi \\
&+ \frac{3}{2}(R-R^{-1})\int_0^{1/R}\xi\boldsymbol{F}\cdot\frac{\mathcal{G}(\boldsymbol{x}-\boldsymbol{\xi})}{8\pi\mu}\,d\xi \\
&- 3(R-R^{-1})\int_0^{1/R}\xi^2\frac{\boldsymbol{F}\times\boldsymbol{d}_{12}}{8\pi\mu}\times\nabla\frac{d\xi}{|\boldsymbol{x}-\boldsymbol{\xi}|}\,. \qquad (10.25)
\end{aligned}
$$

In conclusion, a point force acting transverse to the axis requires an image system consisting of a Stokeslet of strength $(\frac{3}{2}R^{-1}-\frac{1}{2}R^{-3})$, a Stokes dipole of strength $(R^{-2}-R^{-4})$ (which in turn can be further decomposed into a stresslet and rotlet), a rotlet of strength $2R^{-2}(1-R^{-2})$, and a degenerate quadrupole of strength $\frac{1}{4}R^{-1}(1-R^{-2})^2$ — all located at the inverse point, plus an additional distribution of Stokeslets, degenerate quadrupoles, and rotlets along the axis from the sphere center to the inverse point. These integals may be evaluated analytically to give the Oseen's expression for the image [62]. The solution is also given by Higdon [28].[2] In numerical calculations, these integrals over the line segment may be evaluated by Gaussian quadratures, thus effectively reducing the image to a finite number of Stokes singularities at a finite number of quadrature points. As the disturbance Stokeslet is placed further away, *i.e.*, as $R\to\infty$, the inverse point moves towards the sphere center and the line segment collapses onto the sphere center. This then leaves us with the usual situation for the reaction of a sphere to a distant disturbance. On the other hand, if the Stokeslet is very close to the sphere, *i.e.*, $R\approx 1+\epsilon$, the inverse point also moves to a point almost at the sphere surface, *i.e.*, $1/R\approx 1-\epsilon$, and the line distribution extends almost the entire distance from the sphere center to the surface.

Finally, in the limit of vanishingly small separations, the problem reduces to that of a Stokeslet near a plane wall. We start with the line distribution above and expand in a Taylor series *about the inverse point.* We find, as shown Chapter 12, that in the limit of a plane wall the image reduces to lower order Stokes singularities at the inverse point, which are then located exactly at the mirror image of $\boldsymbol{x}_2$.

10.2.4 Image for the Stokeslet Near a Viscous Drop

The image system for a Stokeslet near a spherical viscous drop has been derived by Fuentes *et al.* [16, 17]. Consider a spherical drop of viscosity μ_i immersed in a fluid of viscosity μ_e. As usual, we denote the viscosity ratio by $\lambda=\mu_i/\mu_e$. The derivation of the image system is similar to that given earlier in this chapter for the rigid sphere. The boundary conditions for the rigid sphere are replaced by those for a fluid-fluid interface, *viz.*, the kinematic condition for the radial

[2]There are typographical errors in Higdon's expression for the image but these are easily corrected by dimensional arguments.

velocity, continuity of tangential velocities, and continuity of the tangential component of the surface tractions (see Chapter 4).

For the *axisymmetric* problem of a Stokeslet pointing along the axis, we write the image field, $\boldsymbol{v}^*$, as a multipole expansion,

$$\boldsymbol{v}^* = \frac{F^{\parallel}\boldsymbol{d}_{12}}{8\pi\mu_e}\sum_{n=0}^{\infty}\left\{ A_n^{\parallel}\frac{(\boldsymbol{d}_{12}\cdot\nabla)^n}{n!}\mathcal{G}(\boldsymbol{x}-\boldsymbol{x}_1) + B_n^{\parallel}\frac{(\boldsymbol{d}_{12}\cdot\nabla)^n}{n!}\nabla^2\mathcal{G}(\boldsymbol{x}-\boldsymbol{x}_1)\right\},$$

outside the drop. The interior solution can be written using Lamb's general solution:

$$\begin{aligned}\boldsymbol{v}^{(i)} &= \frac{F^{\parallel}}{8\pi\mu_e}\sum_{n=1}^{\infty}\left\{ a_n^{\parallel}\left[\frac{(n+3)}{2}r_1^{2n+3}\nabla\frac{(\boldsymbol{d}_{12}\cdot\nabla)^n}{n!}\frac{1}{r_1}\right.\right.\\ &\qquad\left. + \frac{(n+1)(2n+3)}{2}r_1^{2n+1}(\boldsymbol{x}-\boldsymbol{x}_1)\frac{(\boldsymbol{d}_{12}\cdot\nabla)^n}{n!}\frac{1}{r_1}\right]\\ &+ b_n^{\parallel}\left.\left[r_1^{2n+1}\nabla\frac{(\boldsymbol{d}_{12}\cdot\nabla)^n}{n!}\frac{1}{r_1} + (2n+1)r_1^{2n-1}(\boldsymbol{x}-\boldsymbol{x}_1)\frac{(\boldsymbol{d}_{12}\cdot\nabla)^n}{n!}\frac{1}{r_1}\right]\right\}.\end{aligned}$$

From the boundary conditions, we obtain a set of four coupled difference equations, which may be solved to yield

$$a_n^{\parallel} = (1-\Lambda)\left[R^{-(n+2)} - R^{-n}\right] \tag{10.26}$$

$$b_n^{\parallel} = -(1-\Lambda)\frac{(n+1)}{2}\left[R^{-(n+2)} - R^{-n}\right] \tag{10.27}$$

$$A_n^{\parallel} = \Lambda\left[\frac{-(2n+3)}{2R^{(n+1)}} + \frac{(2n+1)}{2R^{(n+3)}}\right] - (1-\Lambda)R^{-(n+1)} \tag{10.28}$$

$$B_n^{\parallel} = -\frac{1}{4}\Lambda(1-R^2)^2R^{-(n+5)}\,. \tag{10.29}$$

The parameter $\Lambda = \lambda/(\lambda+1)$ has been introduced to simplify the notation. Note that $0 \le \Lambda \le 1$, with $\Lambda = 0$ corresponding to a bubble and $\Lambda = 1$ to a rigid sphere. We make the following observations about this solution. For $\Lambda = 1$, the expressions above simplify to Equations 10.10 and 10.11, as expected. Note also that the image field for a bubble is particularly simple (we will say more about this later when we examine the singularity form of the image system). Finally, since the solution is linear in Λ, the general solution can be obtained by linear interpolation of the results for a bubble and a rigid sphere!

For the *transverse* problem, outside the drop, we use a multipole expansion,

$$\begin{aligned}\boldsymbol{v}^* &= \frac{\boldsymbol{F}^{\perp}}{8\pi\mu_e}\cdot\sum_{n=0}^{\infty}\left\{ A_n^{\perp}\frac{(\boldsymbol{d}_{12}\cdot\nabla)^n}{n!}\mathcal{G}(\boldsymbol{x}-\boldsymbol{x}_1) + B_n^{\perp}\frac{(\boldsymbol{d}_{12}\cdot\nabla)^n}{n!}\nabla^2\mathcal{G}(\boldsymbol{x}-\boldsymbol{x}_1)\right\}\\ &+ \sum_{n=0}^{\infty}\left\{ C_n^{\perp}\frac{(\boldsymbol{d}_{12}\cdot\nabla)^n}{n!}(\boldsymbol{t}\times\nabla)\frac{1}{r_1}\right\} - (C_0^{\perp} - A_1^{\perp})(\boldsymbol{t}\times\nabla)\frac{1}{r_1}\,,\end{aligned}$$

while inside we have Lamb's solution,

$$\boldsymbol{v}^{(i)} = \sum_{n=1}^{\infty}\left\{ a_n^{\perp}\left[\frac{(n+3)}{2}r_1^{2n+3}\nabla(\boldsymbol{F}\cdot\nabla)\frac{(\boldsymbol{d}_{12}\cdot\nabla)^{n-1}}{n!}\frac{1}{r_1}\right.\right.$$

$$
\begin{aligned}
&+ \frac{(n+1)(2n+3)}{2} r_1^{2n+1} (\boldsymbol{x}-\boldsymbol{x}_1)(\boldsymbol{F}^{\perp}\cdot\nabla)\frac{(\boldsymbol{d}_{12}\cdot\nabla)^{n-1}}{n!}\frac{1}{r_1}\Big] \\
&+ b_n^{\perp}\nabla\left[r_1^{2n+1}(\boldsymbol{F}\cdot\nabla)\frac{(\boldsymbol{d}_{12}\cdot\nabla)^{n-1}}{n!}\frac{1}{r_1}\right] \\
&+ c_n^{\perp}\left[r_1^{2n-1}(\boldsymbol{t}\times\nabla)\frac{(\boldsymbol{d}_{12}\cdot\nabla)^{n-1}}{(n-1)!}\frac{1}{r_1}\right. \\
&\quad \left. + (2n-1)r_1^{2n-3}\boldsymbol{t}\times(\boldsymbol{x}-\boldsymbol{x}_1)\frac{(\boldsymbol{d}_{12}\cdot\nabla)^{n-1}}{(n-1)!}\frac{1}{r_1}\right] .
\end{aligned}
$$

From the boundary conditions, we obtain a set of four coupled difference equations, which may be solved to yield

$$
a_n^{\perp} = \frac{1}{(1+\lambda)}\left[\frac{(n-2)}{(n+1)}R^{-n} - \frac{n}{(n+1)}R^{-(n+2)}\right] \tag{10.30}
$$

$$
b_n^{\perp} = -\frac{(n+1)}{2}a_n^{\perp} + c_{n+1}^{\perp} \tag{10.31}
$$

$$
c_n^{\perp} = \frac{2(2n-3)}{(n-2)(n+(n-3)\lambda)}R^{-(n-1)} \tag{10.32}
$$

$$
\begin{aligned}
A_n^{\perp} &= \Lambda\frac{(2n+1)}{2(n+2)}\left[(n-1)R^{-(n+1)} - (n+1)R^{-(n+3)}\right] \\
&\quad + \frac{(n-1)}{(n+2)}R^{-(n+1)}
\end{aligned} \tag{10.33}
$$

$$
\begin{aligned}
B_n^{\perp} &= \Lambda\left[\frac{(n+1)}{4(n+4)}R^{-(n+5)} - \frac{(n+1)}{2(n+2)}R^{-(n+3)} + \frac{(n-1)}{4(n+2)}R^{-(n+1)}\right] \\
&\quad + \Lambda\frac{(2n+5)(n+1)}{2(n+2)(n+3)(n+4)}\frac{(n+6-3\Lambda)}{(n+4-3\Lambda)}R^{-(n+3)}
\end{aligned} \tag{10.34}
$$

$$
\begin{aligned}
C_n^{\perp} &= \Lambda\frac{(2n+3)}{(n+2)(n+3)}\left[nR^{-(n+2)} - (n+2)R^{-(n+4)}\right] \\
&\quad + \Lambda\frac{2n(2n+3)}{(n+2)(n+3)}\frac{1}{(n+3-3\Lambda)}R^{-(n+2)} .
\end{aligned} \tag{10.35}
$$

Using the same procedure as that employed for the rigid sphere, we may convert the multipole expansion for the image into line distributions. The motivation for this action is as before. For a Stokeslet aligned with $\boldsymbol{d}_{12}$ (the axisymmetric problem), the image is again confined to the inverse point and is given by

$$
\begin{aligned}
\boldsymbol{v}^* &= \left[-\Lambda(\frac{3}{2}R^{-1} - \frac{1}{2}R^{-3}) - (1-\Lambda)R^{-1}\right]\boldsymbol{F}^{\parallel}\cdot\frac{\mathcal{G}(\boldsymbol{x}-\boldsymbol{x}_2^*)}{8\pi\mu_e} \\
&\quad - \Lambda(R^{-2}-R^{-4})F^{\parallel}[(\boldsymbol{d}_{12}\boldsymbol{d}_{12} - \frac{1}{3}\boldsymbol{\delta})\cdot\nabla]\cdot\frac{\mathcal{G}(\boldsymbol{x}-\boldsymbol{x}_2^*)}{8\pi\mu_e} \\
&\quad - \frac{1}{4}\Lambda R^{-1}(1-R^{-2})^2\boldsymbol{F}^{\parallel}\cdot\nabla^2\frac{\mathcal{G}(\boldsymbol{x}-\boldsymbol{x}_2^*)}{8\pi\mu_e} \\
&= \Lambda\boldsymbol{v}_{rigid}^* + (1-\Lambda)\boldsymbol{v}_{bubble}^* .
\end{aligned} \tag{10.36}
$$

The image for the spherical drop is simply a linear combination of the results for the rigid sphere and the bubble ($\Lambda = 0$). As we shall see below, this nice result does not hold in the transverse problem.

For the transverse problem, the image is

$$\begin{aligned}
\boldsymbol{v}^* &= \Lambda \boldsymbol{v}^*_{Rigid} + (1-\Lambda)\boldsymbol{v}^*_{Bubble} \\
&- \frac{3}{2}\Lambda(1-\Lambda)R^{-2}\int_0^{1/R}\Big[R\xi\ L(\xi, 2-3\Lambda) + 2R^2\xi^2 L(\xi, 1-3\Lambda) \\
&\qquad -3R^3\xi^3 L(\xi, -3\Lambda)\Big]\, \boldsymbol{F}^\perp \cdot \nabla^2 \frac{\mathcal{G}(\boldsymbol{x}-\boldsymbol{\xi})}{8\pi\mu_e}\, d\xi \\
&+ 6\Lambda(1-\Lambda)R^{-1}\int_0^{1/R}\Big[R\xi\ L(\xi, 1-3\Lambda) - 3R^2\xi^2 L(\xi, -3\Lambda)\Big] \\
&\qquad \times \frac{\boldsymbol{F}^\perp \times \boldsymbol{d}_{12}}{8\pi\mu_e} \times \nabla \frac{1}{|\boldsymbol{x}-\boldsymbol{\xi}|}\, d\xi\ , \qquad (10.37)
\end{aligned}$$

where

$$L(\xi, \epsilon) = \frac{1-(R\xi)^\epsilon}{\epsilon}\ ,$$

and $\boldsymbol{v}^*_{Rigid}$ and $\boldsymbol{v}^*_{Bubble}$ are given by

$$\begin{aligned}
\boldsymbol{v}^*_{Rigid} &= -(\frac{3}{2}R^{-1} - \frac{1}{2}R^{-3})\boldsymbol{F}^\perp \cdot \frac{\mathcal{G}(\boldsymbol{x}-\boldsymbol{x}_2^*)}{8\pi\mu_e} \\
&+ (R^{-2} - R^{-4})\, \boldsymbol{F}^\perp(\boldsymbol{d}_{12}\cdot\nabla)\cdot \frac{\mathcal{G}(\boldsymbol{x}-\boldsymbol{x}_2^*)}{8\pi\mu_e} \\
&+ \frac{1}{4}R^{-1}(1-R^{-2})^2 \boldsymbol{F}^\perp \cdot \nabla^2 \frac{\mathcal{G}(\boldsymbol{x}-\boldsymbol{x}_2^*)}{8\pi\mu_e} \\
&+ 2R^{-2}(1-R^{-2})\frac{\boldsymbol{F}^\perp \times \boldsymbol{d}_{12}}{8\pi\mu_e} \times \nabla \frac{1}{|\boldsymbol{x}-\boldsymbol{x}_2^*|} \\
&+ \frac{3}{2}(R-R^{-1})\int_0^{1/R} \xi\ \boldsymbol{F}^\perp \cdot \frac{\mathcal{G}(\boldsymbol{x}-\boldsymbol{\xi})}{8\pi\mu_e}\, d\xi \\
&- \frac{3}{4}(R-R^{-1})\int_0^{1/R}(\xi-\xi^3)\boldsymbol{F}^\perp \cdot \nabla^2 \frac{\mathcal{G}(\boldsymbol{x}-\boldsymbol{\xi})}{8\pi\mu_e}\, d\xi \\
&- 3(R-R^{-1})\int_0^{1/R}\xi^2 \frac{\boldsymbol{F}^\perp \times \boldsymbol{d}_{12}}{8\pi\mu_e} \times \nabla \frac{d\xi}{|\boldsymbol{x}-\boldsymbol{\xi}|} \qquad (10.38)
\end{aligned}$$

$$\boldsymbol{v}^*_{Bubble} = R^{-1}\boldsymbol{F}^\perp \cdot \frac{\mathcal{G}(\boldsymbol{x}-\boldsymbol{x}_2^*)}{8\pi\mu_e} - 3\int_0^{1/R} R\xi\ \boldsymbol{F}^\perp \cdot \frac{\mathcal{G}(\boldsymbol{x}-\boldsymbol{\xi})}{8\pi\mu_e}\, d\xi\ . \qquad (10.39)$$

To summarize, when the point force is directed along the axis, the flow outside the drop is that due to the Stokeslet plus that of the image, with the image consisting of a Stokeslet of strength $\Lambda(\frac{3}{2}R^{-1} - \frac{1}{2}R^{-3}) + (1-\Lambda)R^{-1}$, a stresslet of strength $\Lambda(R^{-2} - R^{-4})$, and a degenerate quadrupole of strength $\frac{1}{4}\Lambda R^{-1}(1-R^{-2})^2$ — all located at the inverse point. When the point force is perpendicular to the z-axis, the image consists of a Stokeslet, a stresslet, a degenerate quadrupole, and a rotlet — all located at the inverse point, plus

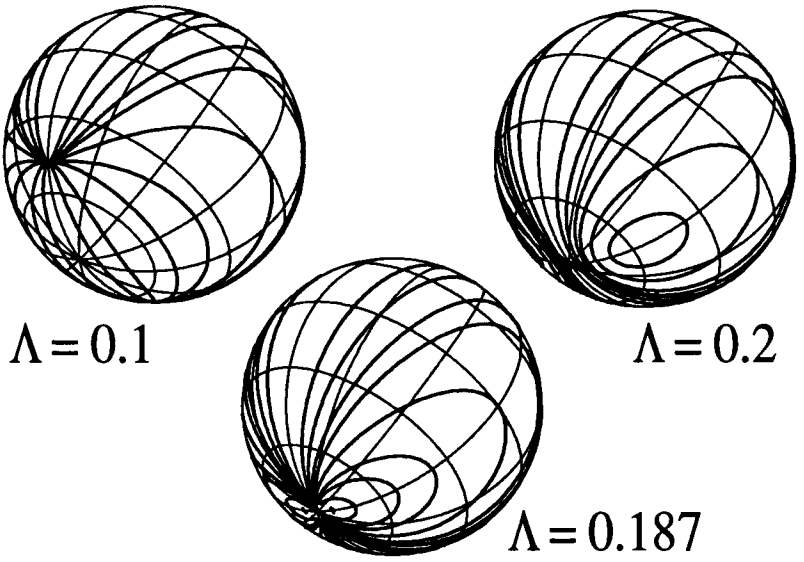

Figure 10.3: Surface flows due to a nearby Stokeslet.

line distributions of Stokeslets, degenerate quadrupoles, and rotlets, from the drop center to the inverse point. The solution for the transverse case is *not* a linear combination of the solutions for the rigid sphere and the bubble. In constrast to the result for rigid spheres, *non-integral* powers of ξ appear in the density functions, the power depending on the viscosity ratio. For $\Lambda = 1/3$ and $\Lambda = 2/3$, *i.e.*, $\lambda = 1/2$ and $\lambda = 2$, we obtain a logarithmic term, because the function $L(\xi, \epsilon)$ becomes the indeterminate form $\lim\{1 - (R\xi)^\epsilon/\epsilon\}$.

Figure 10.3 shows flow lines for the surface velocities induced by the action of a Stokeslet for three different viscosity ratios ($\Lambda = 0.1,\ 0.187,\ 0.2$). The image field was evaluated using the singularity form with Gauss–Jacobi quadratures, with the order of the Jacobi polynomial dictated by Λ. In all three cases, the (transverse) Stokeslet is placed on the z-axis, at $z = 1.2$. These plots show a sequence in which the surface flow field undergoes a change in topology. For relatively inviscid drops, the surface flow field contains two stagnation points that migrate toward the "south pole" with increasing drop viscosity. For $R = 1.2$, at the critical viscosity ratio corresponding to $\Lambda = 0.187$, the stagnation points coalesce. Figure 10.4 shows these critical values as a function of R. For Λ greater than this critical value, the surface of the drop undergoes a "rolling" motion, with centers shifting away from the south pole with increasing viscosity. At values of Λ near unity, this rolling motion is essentially identical to rigid-body rotation, as expected. However, rather curiously, as Λ approached unity, the locus of centers first overshoots the equator, then drifts back. The surface

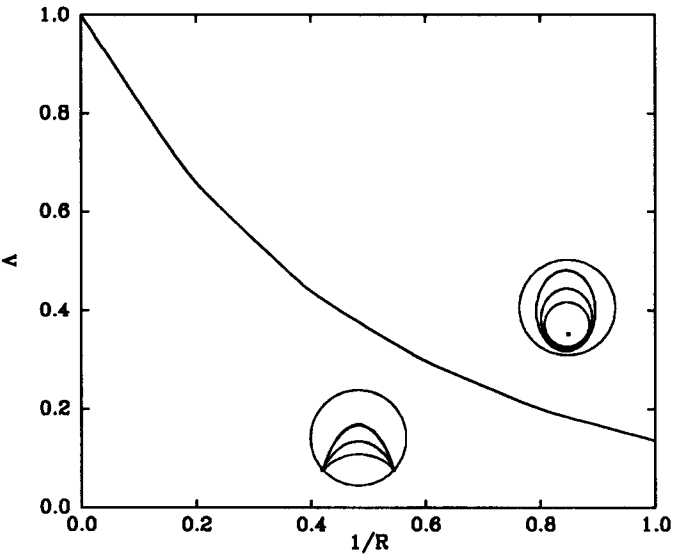

Figure 10.4: Transition to rolling surface motions for the transverse Stokeslet.

flow topology, in particular the presence or absence of the stagnation points, dictates whether surface convection can focus contaminants or surfactants into certain regions.

10.3 Image Systems for Stokes Dipoles

The image system for Stokes dipoles may be obtained by superposition of neighboring Stokeslets of opposite signs and taking the usual limit for a dipole. We effect this mathematically by taking derivatives of the image system for the Stokeslet with respect to $\boldsymbol{x}_2$, the location of the singularity.

Just as $\boldsymbol{F}$ may be decomposed, for axisymmetric geometries, into $\boldsymbol{F}^{\parallel}$ and $\boldsymbol{F}^{\perp}$, the stresslet $\boldsymbol{S}$ too can be written in a special form that exploits the symmetry. Explicitly, we write the stresslet as

$$\begin{aligned}
\boldsymbol{S} &= \boldsymbol{S}^{(0)} + \boldsymbol{S}^{(1)} + \boldsymbol{S}^{(2)} \\
&= \frac{3}{2}(\boldsymbol{d}_{12}\boldsymbol{d}_{12} - \frac{1}{3}\boldsymbol{\delta})\,\boldsymbol{d}_{12}\boldsymbol{d}_{12} : \boldsymbol{S} \\
&+ \boldsymbol{d}_{12}\,(\boldsymbol{S}\cdot\boldsymbol{d}_{12}) + (\boldsymbol{S}\cdot\boldsymbol{d}_{12})\,\boldsymbol{d}_{12} - 2\boldsymbol{d}_{12}\boldsymbol{d}_{12}\,\boldsymbol{d}_{12}\boldsymbol{d}_{12} : \boldsymbol{S} \\
&+ \boldsymbol{S} + \frac{1}{2}\boldsymbol{\delta}\,\boldsymbol{d}_{12}\boldsymbol{d}_{12} : \boldsymbol{S} - \boldsymbol{d}_{12}(\boldsymbol{S}\cdot\boldsymbol{d}_{12}) - (\boldsymbol{S}\cdot\boldsymbol{d}_{12})\boldsymbol{d}_{12} + \frac{1}{2}\boldsymbol{d}_{12}\boldsymbol{d}_{12}\,\boldsymbol{d}_{12}\boldsymbol{d}_{12} : \boldsymbol{S}\ ,
\end{aligned} \tag{10.40}$$

where the labelling indices, $m = 0, 1, 2$ in $\boldsymbol{S}^{(m)} : \boldsymbol{x}\boldsymbol{x}$, correspond to the azimuthal dependence, $e^{im\phi}$, of each stresslet type in polar spherical coordinates about the

axis $\boldsymbol{d}_{12}$ (see Chapter 4 or 5). We consider the three cases separately because they correspond to three distinct operations on the Stokeslet image solution.

10.3.1 The Axisymmetric Stresslet

It may be helpful to keep in mind that the axisymmetric case corresponds to a stresslet whose components may be written as

$$\begin{pmatrix} -1 & 0 & 0 \\ 0 & -1 & 0 \\ 0 & 0 & 2 \end{pmatrix}$$

when the z-axis is taken as the axis of symmetry. The field $(\boldsymbol{S}^{(0)} \cdot \nabla) \cdot \mathcal{G}(\boldsymbol{x} - \boldsymbol{x}_2)$ is equivalent to

$$-(\boldsymbol{d}_{12} \cdot \nabla_2) \frac{3}{2} (\boldsymbol{S} : \boldsymbol{d}_{12}\boldsymbol{d}_{12}) \, \boldsymbol{d}_{12} \cdot \mathcal{G}(\boldsymbol{x} - \boldsymbol{x}_2) \ ,$$

i.e., a dipole formed by two axisymmetric Stokeslets of strength $\frac{3}{2}|\boldsymbol{S}^{(0)} \cdot \boldsymbol{d}_{12}|$ separated along a line parallel to the $\boldsymbol{d}_{12}$ axis, as shown in Figure 10.5. Therefore, the image system for the axisymmetric stresslet, $(\boldsymbol{S}^{(0)} \cdot \nabla) \cdot \mathcal{G}(\boldsymbol{x} - \boldsymbol{x}_2)$, may be obtained by operating on the image system of the axisymmetric Stokeslet with $-(\boldsymbol{d}_{12} \cdot \nabla_2)$. The result is

$$\boldsymbol{v}^* = \sum_{n=0}^{\infty} \left\{ A_n^{(0)} \frac{(\boldsymbol{d}_{12} \cdot \nabla)^n}{n!} \boldsymbol{f} \cdot \frac{\mathcal{G}(\boldsymbol{x} - \boldsymbol{x}_1)}{8\pi\mu} + B_n^{(0)} \frac{(\boldsymbol{d}_{12} \cdot \nabla)^n}{n!} \boldsymbol{f} \cdot \nabla^2 \frac{\mathcal{G}(\boldsymbol{x} - \boldsymbol{x}_1)}{8\pi\mu} \right\} , \quad (10.41)$$

with $\boldsymbol{f} = \boldsymbol{S}^{(0)} \cdot \boldsymbol{d}_{12}$ and

$$\begin{aligned} A_n^{(0)} &= \frac{3}{2} \frac{\partial A_n^{\parallel}}{\partial R} \qquad (10.42) \\ &= \frac{3}{2}(n + \frac{3}{2})(n+1) R^{-(n+2)} - \frac{3}{2}(n + \frac{1}{2})(n+3) R^{-(n+4)} \\ B_n^{(0)} &= \frac{3}{2} \frac{\partial B_n^{\parallel}}{\partial R} \qquad (10.43) \\ &= \frac{3}{8}(n+1) R^{-(n+2)} - \frac{3}{4}(n+3) R^{-(n+4)} + \frac{3}{8}(n+5) R^{-(n+6)} \ . \end{aligned}$$

10.3.2 The Stresslet in Hyperbolic Flow ($m = 1$)

We now consider the stresslet $\boldsymbol{S}^{(1)}$. If the z-axis is taken as the axis of symmetry, the components are proportional to

$$\begin{pmatrix} 0 & 0 & 1 \\ 0 & 0 & 0 \\ 1 & 0 & 0 \end{pmatrix} \quad \text{and} \quad \begin{pmatrix} 0 & 0 & 0 \\ 0 & 0 & 1 \\ 0 & 1 & 0 \end{pmatrix} .$$

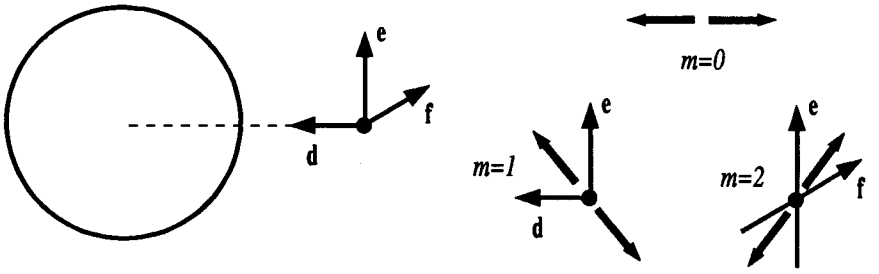

Figure 10.5: Construction of Stokes dipoles from Stokeslets near a sphere.

The two matrices represent the same physical problem if the geometry is axisymmetric about the z-axis. The velocity field $(\boldsymbol{S}^{(1)} \cdot \nabla) \cdot \mathcal{G}(\boldsymbol{x} - \boldsymbol{x}_2)$ is equivalent to

$$-[(\boldsymbol{e}\boldsymbol{d}_{12} + \boldsymbol{d}_{12}\boldsymbol{e}) \cdot \nabla_2] \cdot \mathcal{G}(\boldsymbol{x} - \boldsymbol{x}_2) \ ,$$

where $\boldsymbol{e} = (\boldsymbol{S} \cdot \boldsymbol{d}_{12}) \cdot (\boldsymbol{\delta} - \boldsymbol{d}_{12}\boldsymbol{d}_{12})$ is the component of $\boldsymbol{S} \cdot \boldsymbol{d}_{12}$ that is orthogonal to $\boldsymbol{d}_{12}$. Thus the case $m = 1$ consists of a symmetric sum of two situations: the first corresponding to a Stokes dipole formed by two Stokeslets (directed along $\boldsymbol{d}_{12}$) separated along a direction $\boldsymbol{e}$ perpendicular to $\boldsymbol{d}_{12}$; the second corresponding to a Stokes dipole formed with the roles of $\boldsymbol{d}_{12}$ and $\boldsymbol{e}$ reversed. An antisymmetric combination of these two dipoles would give the image system for the rotlet oriented in the direction $\boldsymbol{e} \times \boldsymbol{d}_{12}$, transverse to the symmetry axis.

Compared to the $m = 0$ case, the $m = 1$ case is "twice the work." The derivations of the image systems for the two Stokes dipole that make up the stresslet $\boldsymbol{S}^{(1)}$ are quite different and we shall examine each in turn.

The Stokes Dipole $(\boldsymbol{e} \cdot \nabla)\, \boldsymbol{d}_{12} \cdot \mathcal{G}(\boldsymbol{x} - \boldsymbol{x}_2)$

This dipole represents the difference between two axisymmetric Stokeslets, the difference taken in a direction orthogonal to the line of centers, as shown in Figure 10.5. Since

$$(\boldsymbol{e} \cdot \nabla_2)\boldsymbol{d}_{12} = -\frac{1}{R}\boldsymbol{e} \ ,$$

the exact relation between the Stokes dipole and the ∇_2 operation follows as

$$\begin{aligned} (\boldsymbol{e} \cdot \nabla)\boldsymbol{d}_{12} \cdot \mathcal{G}(\boldsymbol{x} - \boldsymbol{x}_2) &= -\boldsymbol{d}_{12} \cdot (\boldsymbol{e} \cdot \nabla_2)\mathcal{G}(\boldsymbol{x} - \boldsymbol{x}_2) \\ &= -(\boldsymbol{e} \cdot \nabla_2)\boldsymbol{d}_{12} \cdot \mathcal{G}(\boldsymbol{x} - \boldsymbol{x}_2) - \frac{1}{R}\boldsymbol{e} \cdot \mathcal{G}(\boldsymbol{x} - \boldsymbol{x}_2) \ , \end{aligned}$$

and the desired image system is the sum of two contributions: $-(\boldsymbol{e} \cdot \nabla_2)$ applied to the image system of the axisymmetric Stokeslet and $-\frac{1}{R}$ times the image system of the transverse Stokeslet.

For the first operation, we will need to know that

$$\begin{aligned}
&-(\boldsymbol{e}\cdot\nabla_2)(\boldsymbol{d}_{12}\cdot\nabla)^n\boldsymbol{d}_{12}\cdot\mathcal{G}\\
&= \frac{1}{R}\left[(\boldsymbol{d}_{12}\cdot\nabla)^n\boldsymbol{e}\cdot\mathcal{G}+n(\boldsymbol{d}\cdot\nabla)^{n-1}(\boldsymbol{e}\cdot\nabla)\boldsymbol{d}_{12}\cdot\mathcal{G}\right]\\
&= \frac{1}{R}\left[(n+1)(\boldsymbol{d}_{12}\cdot\nabla)^n\boldsymbol{e}\cdot\mathcal{G}+2n(\boldsymbol{d}_{12}\cdot\nabla)^{n-1}(\boldsymbol{e}\times\boldsymbol{d}_{12})\nabla\frac{1}{r}\right] ,
\end{aligned}$$

where the second step follows from Equation 10.16. The image system for the Stokes dipole $(\boldsymbol{e}\cdot\nabla)\,\boldsymbol{d}_{12}\cdot\mathcal{G}(\boldsymbol{x}-\boldsymbol{x}_2)$ is eventually obtained as

$$\begin{aligned}
\boldsymbol{v}^* = \sum_{n=0}^{\infty}\Big\{&A_n\frac{(\boldsymbol{d}_{12}\cdot\nabla)^n}{n!}\boldsymbol{e}\cdot\frac{\mathcal{G}(\boldsymbol{x}-\boldsymbol{x}_1)}{8\pi\mu}+B_n\frac{(\boldsymbol{d}_{12}\cdot\nabla)^n}{n!}\boldsymbol{e}\cdot\nabla^2\frac{\mathcal{G}(\boldsymbol{x}-\boldsymbol{x}_1)}{8\pi\mu}\\
&+C_n\frac{(\boldsymbol{d}_{12}\cdot\nabla)^n}{8\pi\mu n!}\boldsymbol{t}\times\nabla\frac{1}{r}\Big\} ,
\end{aligned}\tag{10.44}$$

with $\boldsymbol{t}=\boldsymbol{e}\times\boldsymbol{d}_{12}$ and

$$A_n = \frac{(n+1)}{R}A_n^{\parallel}-\frac{1}{R}A_n^{\perp} \tag{10.45}$$

$$B_n = \frac{(n+1)}{R}B_n^{\parallel}-\frac{1}{R}B_n^{\perp} \tag{10.46}$$

$$C_n = \frac{2}{R}A_{n+1}^{\parallel}-\frac{1}{R}C_n^{\perp} . \tag{10.47}$$

The Stokes Dipole $(\boldsymbol{d}_{12}\cdot\nabla)\,\boldsymbol{e}\cdot\mathcal{G}(\boldsymbol{x}-\boldsymbol{x}_2)$

This dipole represents the difference between two transverse Stokeslets, the difference taken in the direction of the line of centers as shown in Figure 10.5, whence its image system is obtained by applying $-(\boldsymbol{d}_{12}\cdot\nabla_2)$ on the transverse Stokeslet $\boldsymbol{e}\cdot\mathcal{G}(\boldsymbol{x}-\boldsymbol{x}_2)$. The result is

$$\begin{aligned}
\boldsymbol{v}^* = \sum_{n=0}^{\infty}\Big\{&A_n\frac{(\boldsymbol{d}_{12}\cdot\nabla)^n}{n!}\boldsymbol{e}\cdot\frac{\mathcal{G}(\boldsymbol{x}-\boldsymbol{x}_1)}{8\pi\mu}+B_n\frac{(\boldsymbol{d}_{12}\cdot\nabla)^n}{n!}\boldsymbol{e}\cdot\nabla^2\frac{\mathcal{G}(\boldsymbol{x}-\boldsymbol{x}_1)}{8\pi\mu}\\
&+C_n\frac{(\boldsymbol{d}_{12}\cdot\nabla)^n}{8\pi\mu\, n!}\boldsymbol{t}\times\nabla\frac{1}{r}\Big\} ,
\end{aligned}\tag{10.48}$$

with $\boldsymbol{t}=\boldsymbol{e}\times\boldsymbol{d}_{12}$ and

$$A_n = \frac{\partial A_n^{\perp}}{\partial R} \tag{10.49}$$

$$B_n = \frac{\partial B_n^{\perp}}{\partial R} \tag{10.50}$$

$$C_n = \frac{\partial C_n^{\perp}}{\partial R} . \tag{10.51}$$

Final Result for Hyperbolic Flow ($m = 1$)

The image system for the stresslet, $(\boldsymbol{S}^{(1)} \cdot \nabla) \cdot \mathcal{G}(\boldsymbol{x} - \boldsymbol{x}_2)$, follows from the sum of the previous two results. We group all terms in the forms $(\boldsymbol{d}_{12}\boldsymbol{e} + \boldsymbol{e}\boldsymbol{d}_{12}) = \boldsymbol{S}^{(1)}$, where $\boldsymbol{e} = \boldsymbol{S}^{(1)} \cdot \boldsymbol{d}_{12}$. It is also helpful to keep in mind that some of the singularities, such as the degenerate quadrupole, are already symmetric with respect to $\{\boldsymbol{d}_{12}, \boldsymbol{e}\}$. The image system is

$$\begin{aligned} \boldsymbol{v}^* &= \sum_{n=0}^{\infty} \Big\{ A_n^{(1)} \frac{(\boldsymbol{d}_{12} \cdot \nabla)^n}{n!} \boldsymbol{e} \cdot \frac{\mathcal{G}(\boldsymbol{x} - \boldsymbol{x}_1)}{8\pi\mu} + B_n^{(1)} \frac{(\boldsymbol{d}_{12} \cdot \nabla)^n}{n!} \boldsymbol{e} \cdot \nabla^2 \frac{\mathcal{G}(\boldsymbol{x} - \boldsymbol{x}_1)}{8\pi\mu} \\ &\quad + C_n^{(1)} \frac{(\boldsymbol{d}_{12} \cdot \nabla)^n}{8\pi\mu\, n!} \boldsymbol{t} \times \nabla \frac{1}{r} \Big\} , \end{aligned} \tag{10.52}$$

with $\boldsymbol{e} = \boldsymbol{S}^{(1)} \cdot \boldsymbol{d}_{12}$, $\boldsymbol{t} = \boldsymbol{e} \times \boldsymbol{d}_{12}$ and

$$A_n^{(1)} = \frac{(n+1)}{R} A_n^{\parallel} + R \frac{\partial}{\partial R} \left(\frac{A_n^{\perp}}{R} \right) \tag{10.53}$$

$$B_n^{(1)} = \frac{(n+1)}{R} B_n^{\parallel} + R \frac{\partial}{\partial R} \left(\frac{B_n^{\perp}}{R} \right) \tag{10.54}$$

$$C_n^{(1)} = \frac{2}{R} A_{n+1}^{\parallel} + R \frac{\partial}{\partial R} \left(\frac{C_n^{\perp}}{R} \right) . \tag{10.55}$$

10.3.3 The Stresslet in Hyperbolic Flow ($m = 2$)

We now consider the last portion, $\boldsymbol{S}^{(2)}$, of the stresslet. When the z-axis is taken as the axis of symmetry, the components are proportional to

$$\begin{pmatrix} 0 & 1 & 0 \\ 1 & 0 & 0 \\ 0 & 0 & 0 \end{pmatrix} \quad \text{and} \quad \begin{pmatrix} 1 & 0 & 0 \\ 0 & -1 & 0 \\ 0 & 0 & 0 \end{pmatrix} .$$

The two matrices represent the same physical problem if the geometry is axisymmetric about the z-axis (one follows from the other by a rotation of 45° about the z-axis). The velocity field $(\boldsymbol{S}^{(2)} \cdot \nabla) \cdot \mathcal{G}(\boldsymbol{x} - \boldsymbol{x}_2)$ is thus equivalent to $-(\boldsymbol{e}\boldsymbol{f} + \boldsymbol{f}\boldsymbol{e}) \cdot \nabla_2) \cdot \mathcal{G}(\boldsymbol{x} - \boldsymbol{x}_2)$, where $\boldsymbol{e}$ and $\boldsymbol{f}$ can be any vectors that form an orthogonal basis for the plane normal to $\boldsymbol{d}_{12}$ (see Figure 10.5). Thus the case $m = 2$ also consists of a symmetric sum of two Stokes-dipoles, but here the role played by $\boldsymbol{e}$ and $\boldsymbol{f}$ are equivalent, so that the solution for the dipole $(\boldsymbol{e} \cdot \nabla)\boldsymbol{f} \cdot \mathcal{G}$ may be obtained by switching $\boldsymbol{e}$ and $\boldsymbol{f}$ in the image system for the dipole $(\boldsymbol{f} \cdot \nabla)\boldsymbol{e} \cdot \mathcal{G}$.

The image system for the Stokes dipole, $(\boldsymbol{f} \cdot \nabla)\boldsymbol{e} \cdot \mathcal{G}(\boldsymbol{x} - \boldsymbol{x}_2)$, can be obtained by applying $(-\boldsymbol{f} \cdot \nabla_2)$ to the image system for the transverse Stokeslet, $\boldsymbol{e} \cdot \mathcal{G}(\boldsymbol{x} - \boldsymbol{x}_2)$. Here, the useful relations are

$$(\boldsymbol{f} \cdot \nabla_2)\boldsymbol{e} = 0 , \qquad (\boldsymbol{f} \cdot \nabla_2)\boldsymbol{d}_{12} = -\frac{1}{R}\boldsymbol{f} , \qquad (\boldsymbol{f} \cdot \nabla_2)R = 0 .$$

After these preliminaries, we obtain the following result for the image system for the Stokes dipole $(\boldsymbol{f}\cdot\nabla)\boldsymbol{e}\cdot\mathcal{G}(\boldsymbol{x}-\boldsymbol{x}_2)$:

$$\begin{aligned}\boldsymbol{v}^* &= \sum_{n=1}^{\infty}\Big\{\frac{A_n^{\perp}}{R}\frac{(\boldsymbol{d}_{12}\cdot\nabla)^{n-1}}{(n-1)!}(\boldsymbol{f}\cdot\nabla)\boldsymbol{e}\cdot\frac{\mathcal{G}(\boldsymbol{x}-\boldsymbol{x}_1)}{8\pi\mu} \\ &\quad + \frac{B_n^{\perp}}{R}\frac{(\boldsymbol{d}_{12}\cdot\nabla)^{n-1}}{(n-1)!}(\boldsymbol{f}\cdot\nabla)\boldsymbol{e}\cdot\nabla^2\frac{\mathcal{G}(\boldsymbol{x}-\boldsymbol{x}_1)}{8\pi\mu}\Big\} \\ &\quad + \sum_{n=0}^{\infty}\frac{C_n^{\perp}}{R}\left[n\frac{(\boldsymbol{d}_{12}\cdot\nabla)^{n-1}}{8\pi\mu n!}(\boldsymbol{f}\cdot\nabla)\boldsymbol{t}\times\nabla\frac{1}{r}+\frac{(\boldsymbol{d}_{12}\cdot\nabla)^{n}}{8\pi\mu n!}(\boldsymbol{e}\times\boldsymbol{f})\times\nabla\frac{1}{r}\right].\end{aligned} \tag{10.56}$$

If we symmetrize this with respect to $\boldsymbol{e}$ and $\boldsymbol{f}$, then the image system for the stresslet $\boldsymbol{S}^{(2)}=\boldsymbol{ef}+\boldsymbol{fe}$ follows as

$$\begin{aligned}\boldsymbol{v}^* &= \sum_{n=0}^{\infty}\Big\{A_n^{(2)}\frac{(\boldsymbol{d}_{12}\cdot\nabla)^n}{n!}(\boldsymbol{S}^{(2)}\cdot\nabla)\cdot\frac{\mathcal{G}(\boldsymbol{x}-\boldsymbol{x}_1)}{8\pi\mu} \\ &\quad + B_n^{(2)}\frac{(\boldsymbol{d}_{12}\cdot\nabla)^n}{n!}(\boldsymbol{S}^{(2)}\cdot\nabla)\cdot\nabla^2\frac{\mathcal{G}(\boldsymbol{x}-\boldsymbol{x}_1)}{8\pi\mu} \\ &\quad + C_n^{(2)}\frac{(\boldsymbol{d}_{12}\cdot\nabla)^n}{8\pi\mu\, n!}[(\boldsymbol{S}^{(2)}\cdot\nabla)\times\boldsymbol{d}_{12}]\times\nabla\frac{1}{r}\Big\},\end{aligned} \tag{10.57}$$

with

$$A_n^{(2)} = \frac{A_{n+1}^{\perp}}{R} \tag{10.58}$$

$$B_n^{(2)} = \frac{B_{n+1}^{\perp}}{R} \tag{10.59}$$

$$C_n^{(2)} = \frac{C_{n+1}^{\perp}}{R}. \tag{10.60}$$

Note that no hydrodynamic force and torque are exerted on the sphere.

10.4 Image System for the Degenerate Stokes Quadrupole

The degenerate quadrupole, $\boldsymbol{F}\cdot\nabla^2\mathcal{G}(\boldsymbol{x}-\boldsymbol{x}_2)$, is an important entity, because it appears in the singularity solution for a sphere (Chapter 3), *i.e.*, the disturbance velocity of a translating sphere of radius b, center at $\boldsymbol{x}_2$ is

$$\boldsymbol{F}\cdot(1+\frac{b^2}{6}\nabla^2)\frac{\mathcal{G}(\boldsymbol{x}-\boldsymbol{x}_2)}{8\pi\mu}. \tag{10.61}$$

We could try a solution approach analogous to the one employed to derive the image system for the Stokes dipole: differentiate the image system of the Stokeslet with respect to $\boldsymbol{x}_2$, the location of the singular point. It turns out however, that this is more work than the direct method, because we have to differentiate twice. In fact, since the degenerate quadrupole is a vector harmonic, the direct analysis is much easier than that for the Stokeslet.

We start with the representation for the degenerate quadrupole:

$$\boldsymbol{F}\cdot\nabla^2\mathcal{G}(\boldsymbol{x}-\boldsymbol{x}_2) \;=\; -2\nabla\boldsymbol{F}\cdot\nabla\frac{1}{r_2}\,. \tag{10.62}$$

We differentiate the Legendre expansion, Equation 10.4, twice with respect to $\boldsymbol{x}_2$ to obtain the following relations for the degenerate quadrupole:

$$\begin{aligned}\nabla\boldsymbol{F}^{\parallel}\cdot\nabla\frac{1}{r_2} \;&=\; -F^{\parallel}\sum_{n=0}^{\infty}\frac{(n+1)(2n+1)}{R^{n+2}}r_1^{2n-1}(\boldsymbol{x}-\boldsymbol{x}_1)\frac{(\boldsymbol{d}_{12}\cdot\nabla)^n}{n!}\frac{1}{r_1}\\ &\quad -\; F^{\parallel}\sum_{n=0}^{\infty}\frac{(n+1)}{R^{n+2}}r_1^{2n+1}\nabla\frac{(\boldsymbol{d}_{12}\cdot\nabla)^n}{n!}\frac{1}{r_1}\end{aligned} \tag{10.63}$$

and

$$\begin{aligned}\nabla\boldsymbol{F}^{\perp}\cdot\nabla\frac{1}{r_2} \;&=\; \sum_{n=0}^{\infty}\frac{(2n+3)}{R^{n+3}}r_1^{2n+1}(\boldsymbol{x}-\boldsymbol{x}_1)(\boldsymbol{F}^{\perp}\cdot\nabla)\frac{(\boldsymbol{d}_{12}\cdot\nabla)^n}{n!}\frac{1}{r_1}\\ &\quad +\; \sum_{n=0}^{\infty}\frac{r_1^{2n+3}}{R^{n+3}}\nabla\,(\boldsymbol{F}^{\perp}\cdot\nabla)\frac{(\boldsymbol{d}_{12}\cdot\nabla)^n}{n!}\frac{1}{r_1}\,.\end{aligned} \tag{10.64}$$

As before, we examine the axisymmetric and transverse cases separately.

10.4.1 The Axisymmetric Problem

We write $\boldsymbol{F}=F\boldsymbol{d}_{12}$ and use Equation 10.63 to express the degenerate quadrupole at $\boldsymbol{x}_2$ in terms of harmonics centered at $\boldsymbol{x}_1$. The image system, $\boldsymbol{v}^*$, is written as a multipole expansion,

$$\boldsymbol{v}^* = \frac{F\boldsymbol{d}_{12}}{8\pi\mu}\cdot\sum_{n=0}^{\infty}\left\{\tilde{A}_n^{\parallel}\frac{(\boldsymbol{d}_{12}\cdot\nabla)^n}{n!}\mathcal{G}(\boldsymbol{x}-\boldsymbol{x}_1)+\tilde{B}_n^{\parallel}\frac{(\boldsymbol{d}_{12}\cdot\nabla)^n}{n!}\nabla^2\mathcal{G}(\boldsymbol{x}-\boldsymbol{x}_1)\right\}.$$

From here on, the analysis is similar to that performed for the Stokeslet problem. The only difference is that when matching the boundary conditions we use terms originating from Equation 10.63 in place of the expression for the Stokeslet. Thus the equations for $\tilde{A}_n^{\parallel}$ and $\tilde{B}_n^{\parallel}$ $(n\geq 1)$ are

$$\begin{aligned}\frac{1}{(2n-1)}\tilde{A}_{n-1}^{\parallel} \;&=\; \frac{(2n+1)}{R^{n+2}}\\ \frac{(n-2)}{(2n-1)}\tilde{A}_{n-1}^{\parallel}-\frac{n}{(2n+3)}\tilde{A}_{n+1}^{\parallel}-2n\tilde{B}_{n-1}^{\parallel} \;&=\; -\frac{2(n+1)}{R^{n+2}}\,,\end{aligned}$$

so that

$$\tilde{A}_n^{\parallel} \;=\; (2n+1)(2n+3)R^{-(n+3)} \tag{10.65}$$

$$\tilde{B}_n^{\parallel} \;=\; \frac{1}{2}(2n+1)R^{-(n+3)}-\frac{1}{2}(2n+7)R^{-(n+5)}\,. \tag{10.66}$$

The hydrodynamic force exerted on the large sphere is

$$\boldsymbol{F}^{\mathrm{Hyd}} = -\tilde{A}_0^{\parallel}F\boldsymbol{d}_{12} = -3R^{-3}F\boldsymbol{d}\,,$$

consistent with the Faxén law. This image system is equivalent to a Stokeslet, stresslet, both degenerate and nondegenerate quadrupoles, and a degenerate octupole — all located at the inverse point.

10.4.2 The Transverse Problem

We now consider the transverse case with $\boldsymbol{F}\cdot\boldsymbol{d}_{12} = 0$. Equation 10.64 will be used to express the singularity at $\boldsymbol{x}_2$ in terms of harmonics at $\boldsymbol{x}_1$. The image system for the transverse case will be the same as that used in the transverse Stokeslet problem: The "three" coefficients — $\tilde{A}_n^{\perp}$, $\tilde{B}_n^{\perp}$, and $\tilde{C}_n^{\perp}$ — are determined from the boundary conditions, which ultimately yields the following set of equations:

$$\begin{aligned}
\left[\, n - 1 - \frac{(2n+1)(n+1)}{(2n+3)} \,\right] \tilde{A}_n^{\perp} &= 2(2n+1)(n+1)R^{-(n+3)} \\
\frac{\tilde{A}_n^{\perp}}{(2n+3)} - \frac{\tilde{A}_{n+2}^{\perp}}{(2n+7)} - 2\tilde{B}_n^{\perp} &= 2R^{-(n+5)} \\
\left[\, 1 - \frac{(2n+3)}{(2n+5)} \,\right] \tilde{A}_{n+1}^{\perp} - \tilde{C}_n^{\perp} &= 2(2n+3)R^{-(n+4)} \,,
\end{aligned}$$

so that

$$\tilde{A}_n^{\perp} = -\frac{(2n+3)(2n+1)(n+1)}{(n+2)}R^{-(n+3)} \tag{10.67}$$

$$\tilde{B}_n^{\perp} = -\frac{(2n+1)(n+1)}{2(n+2)}R^{-(n+3)} + \frac{(n+1)(2n+7)}{2(n+4)}R^{-(n+5)} \tag{10.68}$$

$$\tilde{C}_n^{\perp} = -\frac{2(2n+3)(2n+5)}{(n+3)}R^{-(n+4)} \,. \tag{10.69}$$

The hydrodynamic force and torque exerted by the fluid on the sphere are

$$\boldsymbol{F}^{\mathrm{hyd}} = -\tilde{A}_0^{\perp}\boldsymbol{F} = \frac{3}{2}R^{-3}\boldsymbol{F} \tag{10.70}$$

$$\boldsymbol{T}^{\mathrm{hyd}} = (\tilde{C}_0^{\perp} - \tilde{A}_1^{\perp})\boldsymbol{F}\times\boldsymbol{d}_{12} = 0 \,, \tag{10.71}$$

consistent with the Faxén laws for the force and torque.

This image system may be rewritten as a distribution of singularities consisting of a Stokeslet, a Stokes dipole (which in turn can be further decomposed into a stresslet and rotlet), a rotlet, degenerate and nondegenerate quadrupoles and a degenerate octupole — all located at the inverse point, plus an additional line distribution of Stokeslets, degenerate quadrupoles, and rotlets along the axis from the sphere center to the inverse point.

10.5 Hydrodynamic Interactions Between Large and Small Spheres

The image solutions for Stokes singularites may be employed in method of reflections calculations for the interactions between a large sphere and an arbitrary small particle. The key idea is that over lengths scales associated with the large sphere, the disturbance fields produced by the small particle may be

approximated by those produced by equivalent Stokes singularities. We illustrate this point by examining the interactions between spheres of radii a and b with $\beta = b/a \ll 1$. In the reflections (see Figure 8.1) at the small sphere, we truncate the multipole expansion at the desired order in b/R. For reflections at the large sphere, we retain the entire multipole solution, which of course is the image systems of the Stokes singularities. In the rest of this section, we derive expressions for the mobility functions $x^a_{\alpha\beta}$ to $O(\beta^5)$.

10.5.1 Mobility Functions x_{12} and x^a_{22}

We assume no net force on sphere 1 and a hydrodynamic force $\boldsymbol{F}_2$ on sphere 2, with $\boldsymbol{F}_2 \parallel \boldsymbol{d}_{12}$. The zeroth-order solution is

$$\begin{aligned} 6\pi\mu b\boldsymbol{U}_2^{(0)} &= -\boldsymbol{F}_2 \,, \\ \boldsymbol{v}_2 &= -\boldsymbol{F}_2 \cdot (1 + \frac{b^2}{6}\nabla^2)\frac{\mathcal{G}(\boldsymbol{x} - \boldsymbol{x}_2)}{8\pi\mu} \,. \end{aligned}$$

At sphere 1, the resulting translational motion induced by $\boldsymbol{v}_2$ is, from the Faxén law,

$$\boldsymbol{U}_1^{(1)} = (1 + \frac{a^2}{6}\nabla^2)\boldsymbol{v}_2|_{x=x_1}$$

or

$$6\pi\mu b\boldsymbol{U}_1^{(1)} = -\boldsymbol{F}_2 \left[\frac{3}{2}\left(\frac{b}{R}\right) - \frac{1}{2}\left(\frac{b}{R}\right)\left(\frac{a}{R}\right)^2 - \frac{1}{2}\left(\frac{b}{R}\right)^3\right] \,.$$

Up to this point, the solution procedure is identical to that employed earlier. However, for $\boldsymbol{v}_{12}$ we use the image system for a Stokeslet of strength $\boldsymbol{F}_2$ and a degenerate quadrupole of strength $(b^2/6)\boldsymbol{F}_2$, *for a force-free sphere* at $\boldsymbol{x}_1$. Using results derived earlier in this chapter, we have

$$\begin{aligned} \boldsymbol{v}_{12} &= \boldsymbol{F}_2 \cdot \sum_{n=0}^{\infty} \left\{ A_n \frac{(\boldsymbol{d}_{12}\cdot\nabla)^n}{n!}\frac{\mathcal{G}(\boldsymbol{x}-\boldsymbol{x}_1)}{8\pi\mu} + B_n \frac{(\boldsymbol{d}_{12}\cdot\nabla)^n}{n!}\nabla^2\frac{\mathcal{G}(\boldsymbol{x}-\boldsymbol{x}_1)}{8\pi\mu}\right\} \\ &- \boldsymbol{F}_2 A_0 \cdot \left\{1 + \frac{a^2}{6}\nabla^2\right\}\frac{\mathcal{G}(\boldsymbol{x}-\boldsymbol{x}_1)}{8\pi\mu} \,, \end{aligned}$$

where

$$A_n = A_n^{\parallel} + \frac{b^2}{6}\tilde{A}_n^{\parallel} \,, \qquad B_n = B_n^{\parallel} + \frac{b^2}{6}\tilde{B}_n^{\parallel} \,,$$

with $A_n^{\parallel}$, $B_n^{\parallel}$, $\tilde{A}_n^{\parallel}$, and $\tilde{B}_n^{\parallel}$ given by Equations 10.10, 10.11, 10.65, and 10.66. The image for a force-free sphere is obtained from that of the stationary sphere by placing an additional Stokeslet of opposite sign (and the associated degenerate quadrupole) at $\boldsymbol{x}_1$.

The second reflection result is given by the Faxén law as

$$\boldsymbol{U}_2^{(2)} = (1 + \frac{b^2}{6}\nabla^2)\boldsymbol{v}_{12}|_{x=x_2} \,,$$

and since

$$\begin{aligned}\frac{(\boldsymbol{d}_{12}\cdot\nabla)^n}{n!}\boldsymbol{F}_2\cdot\mathcal{G}(\boldsymbol{x}-\boldsymbol{x}_1)|_{x=x_2} &= 2R^{-(n+1)}\boldsymbol{F}_2\\ \frac{(\boldsymbol{d}_{12}\cdot\nabla)^n}{n!}\boldsymbol{F}_2\cdot\nabla^2\mathcal{G}(\boldsymbol{x}-\boldsymbol{x}_1)|_{x=x_2} &= -2(n+1)(n+2)R^{-(n+3)}\boldsymbol{F}_2\ ,\end{aligned}$$

we obtain

$$\begin{aligned}6\pi\mu b\boldsymbol{U}_2^{(2)} &= -\boldsymbol{F}_2\left\{\left(\frac{b}{R}\right)\left[-\frac{3}{2}x^3+\frac{1}{4}x^5-\frac{9}{4}\sum_{n=1}^{\infty}x^{2n+1}\right]\right.\\ &+ \left(\frac{b}{R}\right)^3\left[\frac{1}{2}x^3+\frac{1}{2}\sum_{n=1}^{\infty}(n+1)(4n+3)x^{2n+1}\right]\\ &- \left.\left(\frac{b}{R}\right)^5\left[\frac{1}{24}\sum_{n=1}^{\infty}(n+1)(n+2)(2n+1)(2n+3)x^{2n+1}\right]\right\}\ ,\end{aligned}$$

with the notation x for a/R.

For the third reflection,

$$\boldsymbol{U}_1^{(3)} = (1+\frac{a^2}{6}\nabla^2)\boldsymbol{v}_{212}|_{x=x_1}\ , \tag{10.72}$$

with

$$\boldsymbol{v}_{212}\sim(\boldsymbol{S}_2^{(2)}\cdot\nabla)\cdot\frac{\mathcal{G}(\boldsymbol{x}-\boldsymbol{x}_2)}{8\pi\mu}\ .$$

Only the axisymmetric component of the stresslet appears in this problem, so it suffices to compute only $\boldsymbol{S}:\boldsymbol{d}_{12}\boldsymbol{d}_{12}$. We apply the Faxén law for the stresslet to the incident field $\boldsymbol{v}_{21}$ and find that

$$\begin{aligned}\boldsymbol{S}_2^{(2)}:\boldsymbol{d}_{12}\boldsymbol{d}_{12} &= \frac{20}{3}\pi\mu b^3\boldsymbol{e}_{21}:\boldsymbol{d}_{12}\boldsymbol{d}_{12}\\ &= \frac{5}{6}b^3\frac{\boldsymbol{F}_2\cdot\boldsymbol{d}_{12}}{R^2}\left[\sum_{n=1}^{\infty}[2(n+1)A_n^{\parallel}x^n-2(n+1)(n+2)(n+3)B_n^{\parallel}x^{n+2}]\right.\\ &\quad\left.-12(B_0^{\parallel}-\frac{1}{6}A_0^{\parallel})x^2\right]\ .\end{aligned}$$

Recall that the last two terms (the $A_0^{\parallel}$ and $B_0^{\parallel}$ terms) are present because the reflection at sphere 1 is for the *force-free* condition. We may now write the stresslet field as

$$(\boldsymbol{S}_2^{(2)}\cdot\nabla)\cdot\mathcal{G}(\boldsymbol{x}-\boldsymbol{x}_2)=\frac{3}{2}[\boldsymbol{S}_2^{(2)}:\boldsymbol{d}_{12}\boldsymbol{d}_{12}](\boldsymbol{d}_{12}\cdot\nabla)\boldsymbol{d}_{12}\cdot\mathcal{G}(\boldsymbol{x}-\boldsymbol{x}_2)\ ,$$

with

$$[\boldsymbol{S}_2^{(2)}:\boldsymbol{d}_{12}\boldsymbol{d}_{12}]\boldsymbol{d}_{12}=\frac{5}{6}\left(\frac{b}{R}\right)^3\left[-4x^2+x^4-3\sum_{n=1}^{\infty}(n+1)x^{2n}\right]a\boldsymbol{F}_2\ .$$

The third reflection contribution, as given by Equation 10.72, thus reduces to the evaluation of the following dipole and octupole fields:

$$\begin{aligned}(\boldsymbol{d}_{12}\cdot\nabla)\boldsymbol{d}_{12}\cdot\mathcal{G}(\boldsymbol{x}-\boldsymbol{x}_2)|_{x=x_1} &= -2R^{-2}\boldsymbol{d}_{12}\\ (\boldsymbol{d}_{12}\cdot\nabla)\boldsymbol{d}_{12}\cdot\nabla^2\mathcal{G}(\boldsymbol{x}-\boldsymbol{x}_2)|_{x=x_1} &= 12R^{-4}\boldsymbol{d}_{12}\ .\end{aligned}$$

Collecting all of the above together, we find that the contribution from the third reflection is

$$6\pi\mu b\boldsymbol{U}_1^{(3)} = -\boldsymbol{F}_2\left(\frac{b}{R}\right)^4\left[\frac{105}{8}x^3-\frac{75}{8}x^5+\frac{15}{8}x^7+\frac{45}{8}\sum_{n=1}^{\infty}x^{2n+1}\right]\ .$$

At the fourth reflection, we have a contribution to the translational velocity of sphere 2, given by

$$\boldsymbol{U}_2^{(4)} = \boldsymbol{v}_{2121}\ ,$$

where $\boldsymbol{v}_{2121}$ is the image for $\boldsymbol{v}212$, which to the desired order of accuracy may be represented by the stresslet field $(\boldsymbol{S}_2^{(2)}\cdot\nabla)\cdot\mathcal{G}(\boldsymbol{x}-\boldsymbol{x}_2)/8\pi\mu$. The Faxén correction, $(b^2/6)\nabla^2\boldsymbol{v}_{2121}$, has been dropped because, as we shall see shortly, it gives a correction of $O(\beta^6)$. From the first part of this chapter we know that for a force-free sphere the image for an axisymmetric stresslet at $\boldsymbol{x}_2$, evaluated at $\boldsymbol{x}_2$, is

$$\begin{aligned}&\frac{3}{2}\left[\frac{\boldsymbol{S}_2^{(2)}}{8\pi\mu}:\boldsymbol{d}_{12}\boldsymbol{d}_{12}\right]\frac{\boldsymbol{d}_{12}}{R^2}\left[\sum_{n=1}^{\infty}[2A_n^{(0)}x^{n-1}-2(n+1)(n+2)B_n^{(0)}x^{n+1}]\right.\\ &\qquad\left.-4x(b_0^{(0)}-\frac{1}{6}a_0^{(0)})\right]\\ &= \frac{3}{2}\left[\frac{\boldsymbol{S}_2^{(2)}}{8\pi\mu}:\boldsymbol{d}_{12}\boldsymbol{d}_{12}\right]\frac{\boldsymbol{d}_{12}}{R^2}\left[4x^3-x^5+3\sum_{n=1}^{\infty}(n+1)x^{2n+1}\right]\ .\end{aligned}$$

We have the expression for $\boldsymbol{S}_2^{(2)}$, and thus an $O(\beta^4)$ contribution from the fourth reflection follows as

$$6\pi\mu b\boldsymbol{U}_2^{(4)} = \boldsymbol{F}_2\left(\frac{b}{R}\right)^4\left(\frac{15}{16}x^2\right)\left[4x^2-x^4+3\sum_{n=1}^{\infty}(n+1)x^{2n}\right]^2\ .$$

Looking back at the steps in the derivation, we see that the occurrence of the perfect square is a consequence of the Lorentz reciprocal theorem. The following expressions for x_{22}^a and x_{12}^a may be obtained by summing contributions from the even and odd reflections, respectively:

$$\begin{aligned}6\pi b x_{12}^a &= \beta\left[\frac{3}{2}x-\frac{1}{2}x^3\right]-\beta^3\left[\frac{1}{2}x^3\right]\\ &+ \beta^4\left[\frac{15}{8}\left(7x^7-5x^9+x^{11}+3\sum_{n=1}^{\infty}x^{2n+5}\right)\right]+O(\beta^6) \qquad (10.73)\\ 6\pi b x_{22}^a &= 1-\beta\left[\frac{3}{2}x^4-\frac{1}{4}x^6+\frac{9}{4}\sum_{n=1}^{\infty}x^{2n+2}\right]\end{aligned}$$

$$+ \beta^3\left[\frac{1}{2}x^6+\frac{1}{2}\sum_{n=1}^{\infty}(n+1)(4n+3)x^{2n+4}\right]$$
$$- \beta^4\left[\frac{15}{16}\left(4x^5-x^7+3\sum_{n=1}^{\infty}(n+1)x^{2n+3}\right)^2\right]$$
$$- \beta^5\left[\frac{1}{24}\sum_{n=1}^{\infty}(n+1)(n+2)(2n+1)(2n+3)x^{2n+6}\right]+O(\beta^6)\ . \quad (10.74)$$

10.5.2 Mobility Functions x_{11} and x_{21}^a

We consider a hydrodynamic force $\boldsymbol{F}_1$ on the larger sphere and none on the smaller sphere (labelled 2). From the reciprocal theorem, $x_{21}^a = x_{12}^a$, and x_{12}^a was derived in the preceding example. Consequently, we consider only x_{11}^a. The leading order contribution is

$$6\pi\mu a\boldsymbol{U}_1^{(0)} = -\boldsymbol{F}_1\ ,$$

while the next correction is given by $\boldsymbol{U}_1^{(2)}$.

Now, terms of the form

$$\left(\frac{b}{R}\right)^N\sum_{n=1}^{\infty}f_n\left(\frac{a}{R}\right)^n$$

will appear only for $N \geq 6$. The $N = 6$ term appears at the fourth reflection and comes from the velocity field of $\boldsymbol{S}_2^{(3)}$, which in turn is proportional to the rate-of-strain of the *image* of the velocity field of $\boldsymbol{S}_2^{(1)}$. Since the solution is desired accurate to $O(\beta^5)$, we will stop after the second reflection.

The following expression for $\boldsymbol{U}_1^{(2)}$ can be obtained from the the expression for $\boldsymbol{U}_2^{(2)}$ of the preceding subsection by switching the labels for the spheres:

$$6\pi\mu\boldsymbol{U}_1^{(2)} = -\boldsymbol{F}_1\left(\frac{a}{R}\right)\left\{\left[-\frac{3}{2}\left(\frac{b}{R}\right)^3+\frac{1}{4}\left(\frac{b}{R}\right)^5-\frac{9}{4}\sum_{n=1}^{\infty}\left(\frac{b}{R}\right)^{2n+1}\right]\right.$$
$$+\left(\frac{a}{R}\right)^3\left[\frac{1}{2}\left(\frac{b}{R}\right)^3+\frac{1}{2}\sum_{n=1}^{\infty}(n+1)(4n+3)\left(\frac{b}{R}\right)^{2n+1}\right]$$
$$\left.-\left(\frac{a}{R}\right)^5\left[\frac{1}{24}\sum_{n=1}^{\infty}(n+1)(n+2)(2n+1)(2n+3)\left(\frac{b}{R}\right)^{2n+1}\right]\right\}\ .$$

We may truncate this expression, retaining terms up to $(b/R)^5$, and the result for x_{11}^a is

$$6\pi a x_{11}^a = 1-\beta^3\left[\frac{15}{4}x^4-\frac{15}{2}x^6+\frac{15}{4}x^8\right]$$
$$-\beta^5\left[2x^6-\frac{33}{2}x^8+\frac{35}{2}x^{10}\right]+O(\beta^6)\ . \quad (10.75)$$

The translational velocity that results from the application of a net external force on the large sphere is given by Stokes law with a small correction of $O(\beta^3)$ due to the presence of the small, force-free sphere.

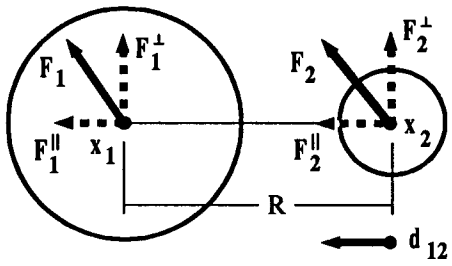

Figure 10.6: Forces and motions for the two-drop geometry.

10.6 Hydrodynamic Interactions Between Large and Small Drops

The preceding discussion on the interactions between large and small *rigid* spheres can be extended to the case of viscous drops, as shown by Fuentes *et al.* [16, 17], the essential modification being the use of the image solutions for a viscous drop in place of that for the rigid sphere. The forces acting on the drops are decomposed into components along and transverse to the axis, and we employ the same notation as used earlier for the rigid spheres (see Figure 10.6).

The final results for the axisymmetric mobility functions $x^a_{\alpha\beta}$ and the asymmetric mobility functions $y^a_{\alpha\beta}$, defined by

$$\begin{pmatrix} \boldsymbol{U}_1^{\parallel} \\ \boldsymbol{U}_2^{\parallel} \end{pmatrix} = \mu^{-1} \begin{pmatrix} x^a_{11} & x^a_{12} \\ x^a_{21} & x^a_{22} \end{pmatrix} \begin{pmatrix} \boldsymbol{F}_1^{\parallel} \\ \boldsymbol{F}_2^{\parallel} \end{pmatrix}$$

$$\begin{pmatrix} \boldsymbol{U}_1^{\perp} \\ \boldsymbol{U}_2^{\perp} \end{pmatrix} = \mu^{-1} \begin{pmatrix} y^a_{11} & y^a_{12} \\ y^a_{21} & y^a_{22} \end{pmatrix} \begin{pmatrix} \boldsymbol{F}_1^{\perp} \\ \boldsymbol{F}_2^{\perp} \end{pmatrix},$$

are

$$\begin{aligned} 6\pi a x^a_{11} &- \frac{3}{2+\Lambda_1} \\ &= -\beta^3 \left[\frac{9\Lambda_2+6}{4} x^4 - \left(\frac{3\Lambda_1}{2+\Lambda_1}\right)\left(\frac{9\Lambda_2+6}{2}\right) x^6 + \frac{3}{4}\left(\frac{3\Lambda_1}{2+\Lambda_1}\right)^2 (7\Lambda_2 - 2) x^8 \right] \\ &- \beta^5 \left[\frac{3(1+\Lambda_2)}{2+\Lambda_2} x^6 - \frac{3}{2}\left(\frac{3\Lambda_1}{2+\Lambda_1}\right)(7\Lambda_2+4) x^8 \right. \\ &\qquad \left. + \frac{5}{2}\left(\frac{3\Lambda_1}{2+\Lambda_1}\right)^2 (9\Lambda_2 - 2) x^{10} \right] \\ &+ O(\beta^6) \end{aligned} \tag{10.76}$$

$$
\begin{aligned}
6\pi b x_{12}^a &= 6\pi b x_{21}^a \\
&= \beta\left[\frac{3}{2}x - \frac{3\Lambda_1}{2(2+\Lambda_1)}x^3\right] - \beta^3\left[\frac{3\Lambda_2}{2(2+\Lambda_2)}x^3\right] \\
&+ \beta^4\left[\frac{3}{8}(2+3\Lambda_2)\left(7\Lambda_1 x^7 - \frac{15\Lambda_1^2}{2+\Lambda_1}x^9 + \frac{9\Lambda_1^3}{(2+\Lambda_1)^2}x^{11}\right.\right. \\
&\qquad \left.\left. + \sum_{n=1}^{\infty}[3\Lambda_1 + 2(1-\Lambda_1)(n+1)]x^{2n+5}\right)\right] + O(\beta^6)
\end{aligned} \tag{10.77}
$$

$$
\begin{aligned}
&6\pi b x_{22}^a - \frac{3}{2+\Lambda_2} \\
&= -\beta\left[\frac{3}{2}\Lambda_1 x^4 - \frac{3\Lambda_1^2 x^6}{4(2+\Lambda_1)} + \frac{3}{4}(2+\Lambda_1)\sum_{n=1}^{\infty}x^{2n+2}\right] \\
&+ \beta^3\left(\frac{3\Lambda_2}{2+\Lambda_2}\right)\left[\frac{\Lambda_1}{2}x^6 + \frac{1}{2}\sum_{n=1}^{\infty}[\Lambda_1(4n+3) + (1-\Lambda_1)(n+2)](n+1)x^{2n+4}\right] \\
&- \beta^4\left[\frac{3}{16}(2+3\Lambda_2)\left(4\Lambda_1 x^5 - \frac{3\Lambda_1^2}{2+\Lambda_1}x^7 + (2+\Lambda_1)\sum_{n=1}^{\infty}(n+1)x^{2n+3}\right)^2\right] \\
&- \beta^5\left(\frac{3\Lambda_2}{2+\Lambda_2}\right)^2\sum_{n=1}^{\infty}\left[\frac{\Lambda_1(2n+3) - 2(1-\Lambda_1)}{24}\right](n+1)(n+2)(2n+1)x^{2n+6} \\
&+ O(\beta^6)
\end{aligned} \tag{10.78}
$$

$$
\begin{aligned}
&6\pi a y_{11}^a - \frac{3}{2+\Lambda_1} \\
&= -\beta^3\frac{1}{4}\left(\frac{3\Lambda_1}{2+\Lambda_1}\right)^2(3\Lambda_2+2)x^8 \\
&+ \beta^5\left[\frac{3}{8}\left(\frac{\Lambda_2^2}{2(2+\Lambda_2)} - \frac{3\Lambda_2 - 2(1-\Lambda_2) + 3\Lambda_2(1-\Lambda_2)}{4-3\Lambda_2}\right)x^6\right. \\
&\left. + \frac{3}{8}\left(\frac{3\Lambda_1}{2+\Lambda_1}\right)(\Lambda_2+2)x^8 - \frac{15}{16}\left(\frac{3\Lambda_1}{2+\Lambda_1}\right)^2(5\Lambda_2+2)x^{10}\right] + O(\beta^6)\,.
\end{aligned} \tag{10.79}
$$

$$
\begin{aligned}
6\pi b y_{12}^a &= 6\pi b y_{21}^a \\
&= \beta\left[\frac{3}{4}x + \frac{3\Lambda_1}{4(2+\Lambda_1)}x^3\right] \\
&+ \beta^3\left[\frac{3\Lambda_2}{4(2+\Lambda_2)}x^3\right] \\
&+ \beta^4\left[\frac{3}{16}(2+3\Lambda_2)\left(\frac{3\Lambda_1}{2+\Lambda_1}\right)\left(-\frac{\Lambda_1^2}{(2+\Lambda_1)}x^{11}\right.\right. \\
&\qquad \left.\left. + \sum_{n=1}^{\infty}(2n+3)\frac{\Lambda_1 n + \Lambda_1(1-\Lambda_1)}{n+3-3\Lambda_1}x^{2n+9}\right)\right] + O(\beta^6)
\end{aligned} \tag{10.80}
$$

$$
\begin{aligned}
6\pi b y^a_{22} &- \frac{3}{2+\Lambda_2} \\
&= \beta\left[\frac{3\Lambda_1^2 x^6}{16(2+\Lambda_1)} - \frac{3}{8}\sum_{n=1}^{\infty}\frac{\Lambda_1 3n - (1-\Lambda_1)2n + 3\Lambda_1(1-\Lambda_1)}{n+3-3\Lambda_1}x^{2n+4}\right] \\
&+ \beta^3\left(\frac{3\Lambda_2}{2+\Lambda_2}\right)\left[\frac{1}{8}\sum_{n=1}^{\infty}[\Lambda_1(4n^2+6n-1)+(1-\Lambda_1)2n(n+2)]x^{2n+6}\right] \\
&- \beta^4\left[\frac{9}{64}(2+3\Lambda_2)\left(\frac{\Lambda_1^2}{2+\Lambda_1}x^7 - \sum_{n=1}^{\infty}(2n+3)\frac{\Lambda_1 n + \Lambda_1(1-\Lambda_1)}{n+3-3\Lambda_1}x^{2n+5}\right)^2\right] \\
&- \beta^5\left(\frac{3\Lambda_2}{2+\Lambda_2}\right)^2\sum_{n=1}^{\infty}\left[\frac{\Lambda_1(2n+3)+2(1-\Lambda_1)}{48}\right](n+1)^2(2n+1)x^{2n+6} \\
&+ O(\beta^6)\,. \qquad (10.81)
\end{aligned}
$$

Exercises

Exercise 10.1 The Moments on a Rigid Sphere Induced by a Nearby Stokeslet.

Consider a sphere at $\boldsymbol{x}_1$ with a Stokeslet nearby at $\boldsymbol{x}_2$. The force, torque, and stresslet may be obtained by applying the Faxén laws to the ambient field, $\boldsymbol{F}\cdot\mathcal{G}(\boldsymbol{x}-\boldsymbol{x}_2)/(8\pi\mu)$. Show that for the axisymmetric Stokeslet,

$$
\begin{aligned}
\boldsymbol{F}^{\mathrm{Hyd}} &= \left(\frac{3}{2}R^{-1} - \frac{1}{2}R^{-3}\right)F^{\parallel}\boldsymbol{d}_{12} \\
\boldsymbol{S} &= \left(-\frac{5}{2}R^{-2} + \frac{3}{2}R^{-4}\right)F^{\parallel}\boldsymbol{d}_{12}\boldsymbol{d}_{12}\,,
\end{aligned}
$$

and for the transverse Stokeslet,

$$
\begin{aligned}
\boldsymbol{F}^{\mathrm{Hyd}} &= \left(\frac{3}{4}R^{-1} + \frac{1}{4}R^{-3}\right)\boldsymbol{F}^{\perp} \\
\boldsymbol{T}^{\mathrm{Hyd}} &= R^{-2}\boldsymbol{F}^{\perp}\times\boldsymbol{d}_{12} \\
\boldsymbol{S} &= -\frac{1}{2}R^{-4}(\boldsymbol{F}^{\perp}\boldsymbol{d}_{12} + \boldsymbol{d}_{12}\boldsymbol{F}^{\perp})\,.
\end{aligned}
$$

Exercise 10.2 Derivation of the General Faxén Law for the Moments on a Sphere.

In Chapter 3, we derived the Faxén laws for a particle of arbitary shape by first deriving expressions for the moments for the special ambient flow produced by a nearby Stokeslet. Now that we know the exact result for a sphere in the Stokeslet ambient field, use the developments in Chapter 3 in the reverse order to derive the Faxén Law for the n-th moment,

$$
\oint_S(\boldsymbol{\sigma}\cdot\hat{\boldsymbol{n}})\boldsymbol{\xi}\boldsymbol{\xi}\ldots\boldsymbol{\xi}\,dS(\boldsymbol{\xi})
$$

on a sphere.

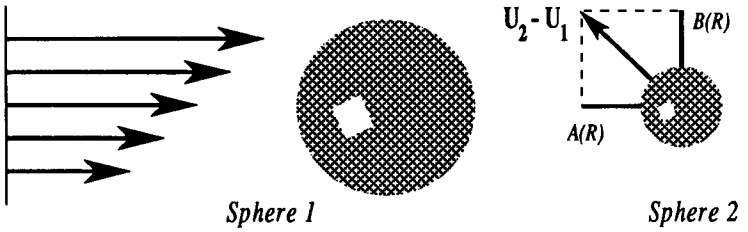

Figure 10.7: Large and small spheres in a linear field.

Exercise 10.3 Two Spheres in a Linear Field.
Consider two neutrally buoyant spheres of radius a and b in the linear ambient field, $\boldsymbol{\Omega}^\infty \times \boldsymbol{x} + \boldsymbol{E}^\infty \cdot \boldsymbol{x}$. Keeping with the theme of this chapter, we assume $\beta = b/a \ll 1$. Use the image system of the stresslet near a rigid sphere to calculate to $O(\beta^5)$ the A and B mobility functions of Batchelor and Green. These were defined in Section 8.4 (see also Exercise 8.6) by the expression

$$\boldsymbol{U}_2 - \boldsymbol{U}_1 = \boldsymbol{\Omega}^\infty \times (\boldsymbol{x}_2 - \boldsymbol{x}_1) + \boldsymbol{E}^\infty \cdot (\boldsymbol{x}_2 - \boldsymbol{x}_1) - [A\boldsymbol{dd} + B(\boldsymbol{\delta} - \boldsymbol{dd})] \cdot \boldsymbol{E}^\infty \cdot (\boldsymbol{x}_2 - \boldsymbol{x}_1) \, .$$

Now consider simple shear flow with sphere centers in the plane of shear. Compute the trajectories of the small sphere for various values of β. How closely do these trajectories follow the streamlines for shear flow past the large sphere in isolation?

Exercise 10.4 Stokeslet Near a Spherical Drop: Surface Deformation.
With a Stokeslet nearby, the shape of a drop is spherical only in the limit of large surface tension γ. For finite surface tensions, we must examine the normal component of the surface tractions and perform a balance between surface tension and hydrodynamic forces. If we take the drop shape to be spherical, what is the error in this force balance? Define an effective capillary number for this problem using the Stokeslet strength F, viscosity μ_e, drop size a, distance between Stokeslet and the drop surface h and surface tension γ. Find the leading corrections to the drop shape (for a history and review of this method, see [9]).